Ionic Conduction and Mechanical Studies on Slide-Ring Gel Electrolytes for Lithium Ion Batteries with Safe and Higher Performance

By Naoki Sugihara

Thesis submitted to
Department of Applied Chemistry,
The Graduate School of Engineering,
Tokyo University of Agriculture and Technology

2016

Table of contents

Preface

Primary batteries are devices taking a Gibbs energy difference (ΔG) out as an electric energy through irreversible or hardly reversible chemical reactions. Because of their simple structures and operation mechanisms, primary batteries represented by dry cells, which cannot be recharged, abound in our daily life. However, using reactions leads to wasting resources, and there are needed for a large-scale recycling center. On the other hand, secondary batteries can charge and discharge the electric energy using the set of reversible chemical reactions, though it needs power sources supplying the activation energy from an external circuit. Since the chemical reactions proceed isothermally, the energetic efficiency with the charging and discharging was considerably large free from the Carnot cycle limitation. Lead storage, nickel-cadmium, and nickel-hydrogen batteries are classified as the secondary batteries.

Electronics, in particular, mobile phone and laptop computer, have great expansion over the world, while are desired to achieve a miniaturization, a weight reduction, and increasing the performance, so that secondary batteries are required to improve the characteristics, such as high voltage, high energy density, and long cycle life. Recently, from the viewpoint of the environmental impact, secondary batteries for vehicles are required to improve. In the three decades, lithium ion batteries (LIBs) are adopted to the battery for meeting these requirements. In the early 1990s, LIBs have become commercial products by Sony and have been used in various products. Nowadays, the market size of LIBs is over 1.5 trillion yen and a lot of investors anticipate that of LIB will grow to 2 trillion yen by 2020.

LIBs are assembled with a cathode, an anode and an electrolyte solution

(ES), however, one of the great problems of LIBs is the liquid state ES with large flowability. Though this flowability has a little problem for safety in the usual condition, it would be the risk of ignition under abnormal heating. Actually, the cases that mobile phones loading LIBs ignited or exploded were happened in the smart phone at 2016. In addition, the using liquid state ES causes leakage and volatilization of ES, hence, many researchers study solidified or pseudo-solidified ESs using polymer matrices.

Solidified or pseudo-solidified ESs are classified into the solid polymer electrolytes (SPEs) and the gel polymer electrolytes (GPEs). SPE is mainly prepared by lithium ion dissolving in poly(ethylene oxide), therefore, SPEs have excellent characteristics, such as no leakage of electrolyte solution, low possibility for ignition, high process ability, because of their liquid-free structure. However, SPEs have a disadvantage that they do not have high ionic conductivity at room temperature for commercial use ($<10^{-4}$ S/cm). Meanwhile, GPEs are prepared by the composition of electrolyte solution and polymer matrix, e.g. poly(vinylidene fluoride-hexafluoropropylene) (PVdF-HFP). GPEs are containing a large amount of liquid in polymer matrices, but the risk of leakage is low because of using the low crystalline HFP for retention of liquid. Thus, GPEs have high ionic conductivity at room temperature and the beginning by Bell Communications Research, Inc., they are commercialized by many company currently. The trade-off between ionic conductivity and mechanical strength is a remaining subject for making higher performance of GPEs, so I focused on a novel kind of gels for applying GPE and aim to achieve the GPE with both the high ionic conductivity and high mechanical strength.

In this thesis, I researched electrochemical and mechanical properties of GPE based on a slide-ring (SR) gel for applying LIB.

Chapter 1

Introduction

1.1 General introduction for lithium ion battery

The improvement of power storage technologies play an important role on the environmental protection imposed on a modern industrial development, furthermore, the requirement of higher performance is significantly increasing from various fields using batteries. Lithium ion battery (LIB) is one of the most efficient forms of power storage facilities and the various characteristics of LIB, e.g. high energy density, high voltage, long cycle life, yield various kinds of electronics to advance. Many kinds of electronics, such as mobile phone, laptop computer, and digital camera, develop into familiar existences by the improvement of LIB and the performance of LIB decides that of electric vehicle and smart grids that come to the fore in next generation. Consequently, we have no doubt that the improvement of LIB influences on the quality of our life.

Transition metals oxides or active sulfur ($LiCoO_2$ [1-3], $LiMn_2O_4$ [1-2,4-5], $LiNO_2$ [1,3], or S_8 [6] at cathode and graphite [7-8] at anode are commonly used as electrodes of present LIB. Cathode and anode are separated by stretching polymer film with sub-micro pores filled with electrolyte solution (ES). ESs typically consist of organic solvents, propylene carbonate (PC) [9-11], ethylene carbonate (EC) [11] and dimethyl carbonate (DMC) [12], including lithium ion, $LiPF_6$ [9], $LiBF_4$ [13], and $Li(CF_3SO_2)_2N$ (LiTFSI) [1,10]. The separator and ES carry lithium ions during the charge and discharge process and prevent the cathode and anode from physical contacts. Figure 1-1 illustrates the schematic of electrochemical reaction in the basic LIB using $LiCoO_2$ cathode and graphite anode. During the charge process, the lithium cations are extracted from the cathode layer and are inserted into the anode layer after migrated in the ES. During the discharge process, lithium cations are

inserted into the cathode layer by reverse reaction. Therefore, LIBs are also called "rocking chair battery" because lithium ions shuttle between cathode and anode in both charge and discharge process. For example, LIB consisting of above materials operates at around 4 V, and has a specific energy of 160 Wh/kg [14]. Operating voltage is provided by the difference between the chemical potential of cathode and anode, therefore, the cathode of $LiMnCoO_4$, which can offer 5 V, has been developed recently [15].

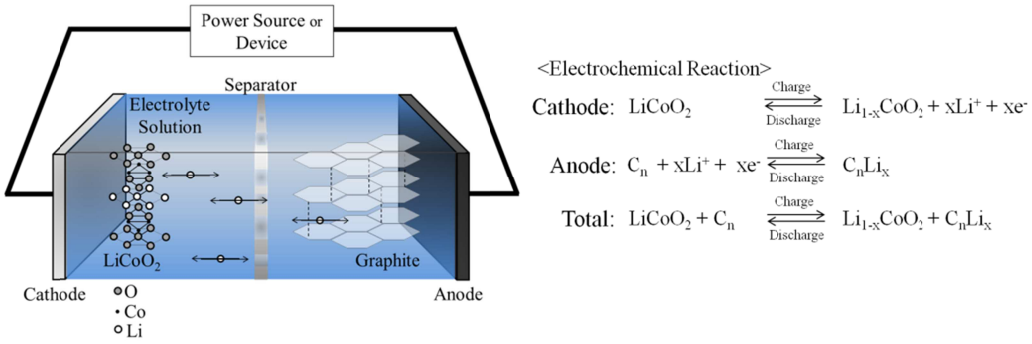

Figure 1-1. Schematic of the electrochemical reaction of a lithium ion battery using $LiCoO_2$ cathode and graphite anode.

To satisfy requirement of high operating voltage needs for electrolyte solution to have high potential window, i.e., LUMO of electrolyte is higher than the chemical potential of an anode and HOMO of electrolyte is lower than the chemical potential of a cathode. In addition, the anode is covered by a thin layer, called solid–electrolyte interphase, which is formed between lithium ions and organic compounds produced by a reductive decomposition. The solid–electrolyte interphase decreases the operational voltage by increasing the chemical potential of the anode, while the solid–electrolyte interphase has a role of preventing decomposition of

electrolyte solution on the anode. Incidentally, a lithium dendrite grows on the cathode during the charge and discharge cycle. The lithium dendrite has a potential hazard leading to ignition by the internal short circuit and reducing a cycle life.

1.2. Separators

Commonly, separator films are used stretching polymer films having a high mechanical strength and polyolefin based polymers, i.e., polyethylene (PE), polypropylene (PP) and a copolymer of PE and PP are typically used for separators of commercial LIB [16-21]. Ionic conductivities of all separators filled with ES have more than 1.0×10^{-3} S/cm and a measurable mechanical strength. Separator films with less than this ionic conductivity are not able to use for LIB and films with an insufficient mechanical strength are also difficult to manufacture LIB. These separators have a disadvantage of poor solvent retaining property. Therefore, in LIBs based on these separators, some metal parts have to be used for preventing leakage of ES, but these metal parts often conflict with the requirements of weight saving and miniaturization.

1.3. Polymer electrolytes

Polymer electrolytes have been developed to improve this problem and there are two kinds of polymer electrolytes, solid polymer electrolyte (SPE) [22-23] and gel polymer electrolyte (GPE) [24]. SPEs are made by polymer matrices and lithium salts without any liquids. Therefore, SPEs have high safety, reliability and

lightness, whereas, ionic conductivities are less than 1.0×10^{-4} S/cm at room temperature. Hence, LIBs with SPE have not made practicable yet. On the other hand, GPEs are also composed of ESs and polymer matrices, polymers become swollen gel by physical cross-linking or chemical cross-linking. Ionic conductivities of GPEs are more than 1.0×10^{-3} S/cm at room temperature. Thus LIBs using GPEs for ES are commercialized by some companies.

1.3.1. General gel polymer electrolytes

Gel polymer electrolytes (GPEs) have been developed to satisfy above requirements and to decrease internal resistance by a large amount of ES in the polymer matrix. Generally, GPEs approximately divided into an entangled linear polymer electrolyte and a cross-linked polymer gel electrolyte. Polyacrylonitrile (PAN) [25-33], poly(methyl methacrylate) (PMMA) [34-39] and poly(vinylidene fluoride-hexafluoropropylene) (PVdF-HFP) [40-47] belong to the entangled linear polymer electrolyte and poly(ethylene oxide) (PEO) [1,10], poly(propylene oxide) (PPO) [48-49] and polyurethane [50] belong to the cross-linked polymer gel electrolyte. Figure 1-2 illustrates the structures of the entangled linear polymer electrolyte and the cross-linked polymer gel electrolyte. The entangled linear polymer electrolytes are prepared by dissolving polymers in ES and polymers are physically cross-linked each other to keep their bulky volume. Manufacturing method of these GPEs is simple, however, these GPEs have poor stability against temperature and pH, and ES containing ratio is generally low. Meanwhile, the cross-linked polymer gel electrolytes are prepared by a photochemical or thermal polymerization to have chemical cross-linkage. These GPEs have good stability

against temperature and pH, however manufacturing method of these GPEs is complicated and some GPEs have poor mechanical strength. Therefore, we have to consider the manufacturing method of GPEs from these advantages and disadvantages. Furthermore, the performances of GPEs should be always compared to that of pristine ESs. For example, the ionic conductivity decreases by one third to half under polymerization (figure 1-3). So that, by preventing ionic conductivity from decrease under polymerization, it can be expected to realize higher performance LIB. Table 1-1 shows the requirement for GPEs [51].

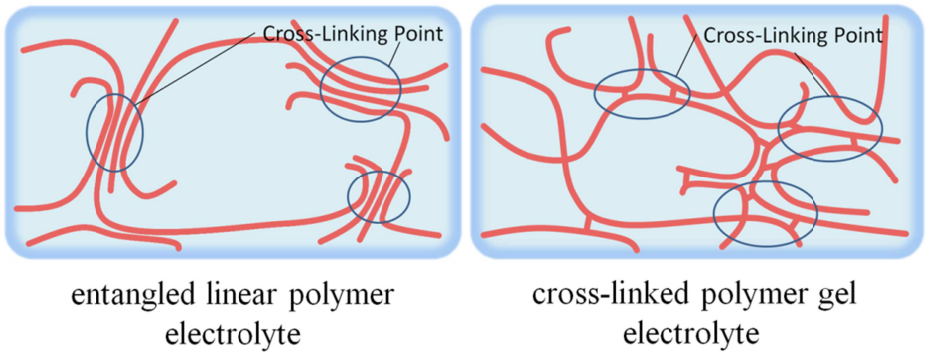

Figure 1-2. Structures of common gels.

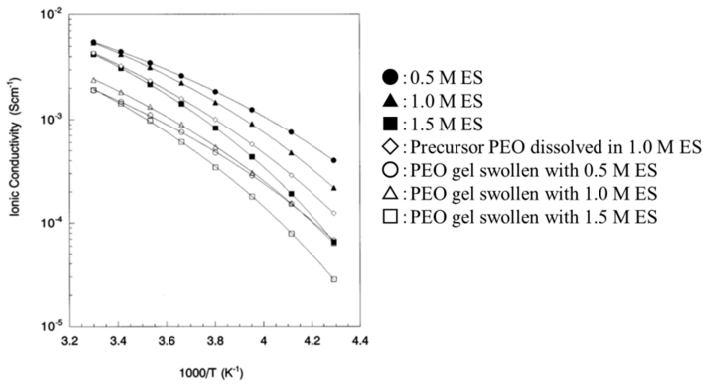

Figure 1-3. Decreasing ionic conductivity by polymerization [10].

Table 1-1. The demand characteristics for GPEs [51].

	Demand characteristics
Ionic conductivity	More than 10^{-3} S/cm at room temperature
Potential window	More than 4.8 V
Interface	100% contact holding
Stability	Retaining gel condition from –20℃ to 100℃
Mechanical strength	Growth suppressing of lithium dendrite
Environmental safety	No problems from manufacturing to incineration
Cost	Less than the sum of separator and ES

1.3.2. Poly(vinylidene fluoride)

Poly(vinylidene difluoride) (PVdF) and PVdF-HFP are typical crystalline polymer and these are obtained the structure of physical gel by several methods. GPEs based on these polymers are typically manufactured by solvent evaporation technique. These polymers are dissolved in the heated mixture of ES and volatile solvent which has compatibility with these polymers, such as N-methylpyrrolidone and 2-butanone, and these mixtures are cooled with the evaporation of volatile solvent. After that GPEs based on these polymers are obtained [52]. The compatibility of volatile solvent to polymers affects the morphology of polymeric structure which influences the property of GPE through the amount of retaining ES in the gel. PVdF-HFP is frequently used as commercial GPE because of the characteristics of good stability against thermally and chemical stress. However, PVdF-HFP has disadvantages, such as poor retention with ES and weak adhesive strength.

1.3.3. Polyether

Polyether resins, such as PEO, PPO, and copolymers of PEO and PPO for GPEs are used for GPE. GPEs based on polyether resins are obtained by the thermo- or photo-radical polymerization of polyether oligomer with methacrylate or acrylate group and they have chemical cross-linkings [53-54]. The GPE based on polyether resin has approximately 0.4 MPa tensile strength and high retention for ES. However, the ionic conduction is disturbed by the interaction between polymer matrices, solvent and lithium cations [53].

1.4. Structures and properties of slide-ring gel

1.4.1. Polyrotaxane

Many researchers focus on polymeric supramolecules in which molecules interacted by noncovalent bonds, such as hydrogen bond, van der Waals interaction, hydrophobic interaction, or π–π interaction [55-56]. Polyrotaxane (PR) is one of the polymeric supramolecule [57]. The structure has a plurality of cyclic molecules, α–cyclodextrins (α–CD), and they are penetrated by an axial polymer chain, polyethylene glycol (PEG), capped by the bulky end groups at the both ends. The polyrotaxane has potentially modifying hydroxyl groups on CDs. α–CD has three hydroxyl groups per one glucose residue, that is, totally 18 hydroxyl groups, and hydroxyl group on α–CD has a chemical reactivity. Hence, various derivatives of PR were also reported. Derivatives of PR have quite different solvent affinity from original PR [59]. For example, original PR does not show affinity for water, because α–CDs on PR form strong hydrogen bonds with inter- and intra-molecules and

aggregate each other. On the other hand, methylated PR (MePR) and hydroxypropylated PR (HyPR) have good affinity for water. This is because the bulky side group of CDs hinder the hydrogen bonding [59].

1.4.2. Slide-ring gel

In section 1.2.1, we explained the structure and characteristics of conventional gels. Meanwhile, slide-ring (SR) gel was reported by Okumura and Ito in 2001 [60]. SR gel is also called a "topological gel", and the structure shows in figure 1-4.

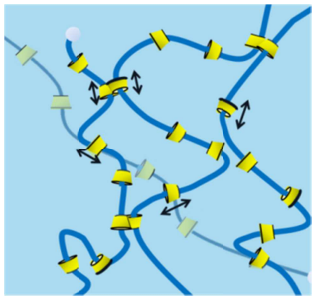

Figure 1-4. Structure of SR gel.

SR gel is prepared by chemically intermolecular cross-linking of PRs and SR gel has "figure of 8 cross-links". The cross-linking junction is not fixed on an axial polymer chain by chemical and physical interaction, therefore, can move freely[61-63].

Chemical gels have a fixed cross-linking junction by covalent bond, therefore, the local polymer density of the network structure is not uniform even in the equilibrium state. As a result, lowering the mechanical strength occurs by the stress concentration to a polymer chain with short distances between cross-linking

junctions under stretching. However, mobile cross-linking junctions of SR gel can prevent the stress concentration to polymer chain with short distances between cross-linking junctions. Thus, SR gel has high mechanical strength and unique mechanical properties [60,64-67]. In addition, SR gel was reported the characteristics of high swelling ratio, high toughness, environmental safety and transparency [65]. Using the SR gel for GPE is expected to be applied to some devices which are required for having the bending and stretching properties, such as wearable devices and card type devices. Furthermore, thinner SR gels is expected for a novel type of the GPE separator with a higher energy density as a substitution of the common GPEs.

References

[1] J. M. Tarascon, M. Armand, Issues and challenges facing rechargeable lithium batteries, 414 (2001) 359-367.

[2] J. B. Bates, N. J. Dudney, B. Neudecker, A. Ueda. C. D. Evans, Thin-film lithium and lithium-ion batteries, Sol. St. Ion. 135 (2000) 33-45.

[3] T. Ohzuku, A. Ueda, M. Nagayama, Y. Iwakoshi, H. Komori, Comapative study of $LiCoO_2$, $LiNi_{12}Co_{12}O_2$ and $LiNiO_2$ for 4 volt secondary lithium sells, Electrochim. Acta 38 (1993) 1159-1167.

[4] Y. Y. Xia, M. Yoshio, An investigation of lithium ion insertion into spinel structure Li-Mn-O compounds, J. Electrochem. Soc. 143 (1996) 825-833.

[5] A. R. Armstrong, P. G. Bruce, Synthesis of layered $LiMnO_2$ as an electrode for rechargeable lithium batteries, Nature 381 (1996) 499-500.

[6] B. S. Kim, S. M. Park, In Situ spectroelectrochemical studies on the reduction of sulfur in dimethyl sulfoxide solutions, J. Electrochem. Soc. 140 (1993) 115-122.

[7] C. K. Chan, H. L. Peng, G. Liu, K. McIlwrath, X. F. Zhang, R. A. Huggins, Y. Cui, High-performance lithium battery anodes using silicon nanowires, Nature Nanotech. 3

(2008) 31-35.
[8] N. Imanishi, S. Ohashi, T. Ichikawa, Y. Takeda, O. Yamamoto, R. Kanno, Carbon lithium anodes for lithium secondary batteries, 39 (1992) 185-191.
[9] S. S. Zhang, A review on electrolyte additives for lithium-ion batteries, 162, (2006) 1379-1394.
[10] Y. Aihara, S. Arai, K. Hayamizu, Ionic conductivity, DSC and self diffusion coefficients of lithium, anion, polymer, and solvent of polymer gel electrolytes: the structure of the gels and the diffusion mechanism of the ions, Electrochim. Acta 45 (2000) 1321-1326.
[11] V. Etacheri, R. Marom, R. Elazari, G. Salitra, D. Aurbach, Challenges in the development of advanced Li-ion batteries: a review, 4 (2011) 3243-3262.
[12] B. Schaffner, F. Schaffner, S. P. Verevkin, A. Borner, Organic carbonates as solvent in synthesis and catalysis, Chem. Rev. 110 (2010) 4554-4581.
[13] S. Rajendran, T. Uma, Lithium ion conduction in PVC-$LiBF_4$ electrolytes gelled with PMMA, J. Pow. Sources 88 (2000) 282-285.
[14] B. Z. Jang, C. G. Liu, D. Neff, Z. N. Yu, M. C. Wang, W. Xiong, A. Zhamu, Graphene surface-enabled lithium ion-exchanging cells: next-generation high-power energy storage devices, 11 (2011) 3785-3791.
[15] M. Michalska, B. Hamankiewicz, D. Ziolkowska, M.Krajewski, L. Lipinska, M. Andrzejczuk, A. Czerwinski, Influence of LiMn2O4 modification with CeO2on electrode performance, 136 (2014) 286-291.
[16] H. S. Bierenbaum, R. B. Issacson, M. L. Druin, S. G. Plovan, Microporous polymeric films, Ind. Eng. Chem. Prod. Res. Dev., 13 (1974) 2-9.
[17] C. R. Jarvis, W. J. Macklin, A. J. Macklin, N. J. Mattingley, E. Karonfli, Use of grated PVdf-based polymers in lithium batteries, J. Power Sources 97-98 (2001) 664-666.
[18] Y. M. Lee, J. W. Kim, N. S. Choi, J. A. Lee, W. H. Seol, J. K. Park, Novel porous separator based on PVdF and PE non-woven matrix for rechargeable lithium batteries, J. Power Sources 139 (2005) 235-241.
[19] Z. Jiang, B. Carroll, K. M. Abraham, Studies of some poly(vinylidene fluoride) electrolytes, Electrochim. Acta 42 (1997) 2667-2677,
[20] S. S Choi, Y. S. Lee, C. W. Joo, S. G. Lee, J. K. Park, K. S. Han, Electrospun PVDF nanofiber web as polymer electrolyte or separator, Electrochim. Acta 50 (2004) 339-343.
[21] M. Armand, The history of polymer electrolytes, Sol. St. Ion. 69 (2002) 309-319.
[22] J. W. Fergus, Ceramic and polymeric solid electrolytes for lithium-ion batteries, 195 (2010) 4554-4569.

[23] K. Kimura, J. Hassoun, S. Panero, B. Scrosatio, Y. Tominaga, Electrochemical properties of a novel poly(ethylene carbonate)-LiTFSI electrolyte containing a pyrrolidinium-based ionic liquid, Ionics 21 (2015) 895-900.
[24] J. Y. Song, Y. Y. Wang, C. C. Wan, Review of gel-type polymer electrolytes for lithium-ion batteries, J. Power Sources 77 (1999) 183-197.
[25] M. Watanabe, M. Kanba, K. Nagaoka, I. Shinohara, Ionic conductivity of hybrid films based on polyacrylonitrile and their battery application, J. Appl. Polym. Sci. 27 (1982) 4191-4198.
[26] K. M. Abraham, M. Alamgir, Li^+-conductive solid polymer electrolytes with liquid-like conductivity, J. Electrochem. Soc. 137 (1990) 1657-1658.
[27] H. Akashi, K. Sekai, K. Tanaka, A novel fire-retardant polyacrylonitrile –based gel electrolyte for lithium batteries, Electrochem. Acta 43 (1998) 1193-1197.
[28] S. Slane, M. Salomon, Composite gel electrolyte for rechargeable lithium batteries, J. Power Sources 55 (1995) 7-10.
[29] H.R. Jung, D. H. Ju, W. J. Lee, X. W. Zhang, R. Kotek, Electrospun hydrophilic fumed silica/polyacrylonitrile nanofiber-based composite electrolyte membranes, Electrochim. Acta 54(2009) 3630-3637.
[30] A. I. Gopalan, P. Santhosh, K. M. Manesh, J. H. Nho, S. H. Kim, C. G. Hwang, K. P. Lee, Development of electrospun PVdF-PAN membrane-based polymer electrolytes for lithium batteries, J. Membr. Sci. 325 (2008) 683-690.
[31] B. Y. Huang, Z. X. Wang, L. Q. Chen, R. J. Xue, F. S. Wang, The mechanism of lithium ion transport in polyacrylonitrile-based polymer electrolytes, Sol. St. Ion. 91 (1996) 279-284.
[32] T. Osaka, T. Momma, H. Ito, B. Scrosati, Performances of lithium/gel electrolyte/polypyrrole secondary batteries, J. Power Sources 68 (1997) 392-396.
[33] S. Mitra, A. K. Shukla, S. Sampath, Electrochemical capacitors with plasticized gel-polymer electrolytes, J. Power Sources 101 (2001) 213-218.
[34] O. Bohnke, M. Frand, M. Rezrazi, C. Rousselot, C. Truche, Fast ion transport in new lithium electrolytes gelled with PMMA. 2. influence of polymer concentration, Sol. St. Ion. 66 (1993) 105-112.
[35] P. E. Stallworth, S. G. Greenbaum, F. Croce, S. Slane, M. Salomon, Lithium-7 NMR and ionic conductivity studies of gel electrolytes based on poly(methylmethacrylate), Electrochim, Acta 40 (1995) 2137-2141.
[36] F. Croce, S. D. Brown, S. G. Greenbaum, S. M. Slane, M. Salomon, Lithium-7 NMR and ionic conductivity studies of gel electrolytes based on polyacrylonitrile, Chem. Mater. 5 (1993) 1268-1272.

[37] J. Vondrak, M. Sedlarikova, J. Velicka, B. Klapste, V. Novak, J. Reiter, Gel polymer electrolytes based on PMMA, Electrochim. Acta 46 (2001) 2047-2048.
[38] H. P. Zhang, P. Zhang, Z. H. Li, M. Sun, Y. P. Wu, H. Q. Wu, A novel sandwiched membrane as polymer electrolyte for lithium ion battery, Electrochem. Commun. 9 (2007) 1700-1703.
[39] S. Rajendran, T. Uma, Lithium ion conduction in PVC-$LiBF_4$ electrolytes gelled with PMMA, J. Power Sources 88 (2000) 282-285.
[40] C. Capiglia, Y. Saito, H. Kataoka, T. Kodama, E. Quartarone, P. Mustarelli, Structure and transport properties of polymer gel electrolytes based on PVdF-HFP and$Li(C_2F_5SO_2)_2$, Sol. St. Ion. 131 (2001) 291-299.
[41] A. M. Stephan, S. G. Kumar, N. G. Renganathan, M. A. Kulandainathan, Characterization of poly(vinylidene fluoride-hexafluoroprplylene) (PVdF-HFP) electrolytes complexed withdifferent lithium salts, Eur. Polym. J. 41 (2005) 15-21.
[42] A. M. Stephan, K. S. Nahm, M. A. Kulandianathan, G. Ravi, J. Wilson, Poly(vinilidene fluoride-hexafluoropropylene) (PVdF-HFP) based composite electrolytes for lithium batteries, Eur. Polym. J. 42 (2006) 1728-1734.
[43] D. Saika, A. Kumar, Ionic conduction in P(VDF-HFP)/PVDF-(PC+DEC)-$LiCLO_4$ polymer gel electrolytes, Electrochim. Acta 49 (2004) 2581-2589.
[44] H. S. Kim, S. I. Moon, Electrochemical properties of the Li-ion polymer batteries with P(VDF-co-HFP)-based gel polymer electrolyte, J. Power Sources 141 (2005) 293-297.
[45] S. Abbrent, J. Plestil, D. Hlavata, J. Lindgren, J. Tegenfeldt, A. Wendsjo, Crystallinity and morphology of PVdF-HFP-based gel electrolytes, Polymer 42 (2001) 1407-1416.
[46] Z. H. Li, G. Y. Su, X. Y. Wang, D. S. Gao, Micro-porous P(VDF-HFP)-based polymer electrolyte filled with Al_2O_3 nanoparticles, Sol. St. Ion. 176 (2005) 1903-1908.
[47] W. H. Pu, X. M. He, L. Wang, C. Y. Jiang, C. R. Wan, Preparation of PVDF-HFP microporous membrane for Li-ion batteries by phase inversion, J. Membr. Sci. 272 (2006) 11-14.
[48] Z. Y. Cui, Y. Y. Xu, L.P. Zhu, J. Y. Wang, Z. Y. Xi, B. K. Zhu, Preparation of PVDF/PEO-PPO-PEO blend microporous membranes for lithium ion batteries via thermally induced phase separation, J. Membr. Sci. 325 (2008) 957-963.
[49] P. Jannasch, Ion conducting electrolytes based on aggregating comblike poly(propylene oxide), Polymer 42 (2001) 8629-8635.
[50] P. Santhosh, T. Vasudevan, A. Gopalan, K. P. Lee, Preparation and properties of new cross-linked polyurethane acrylate electrolytes for lithium batteries, J. Power

Sources 160 (2006) 609-620.
[51] 植谷慶雄 (1999) ポリマーリチウム電池 シーエムシー出版
[52] E. Garcia-Tamayo, M. Valvo, U. Lafont, C. Locati, D. Munao, E. M. Kelder, Nanostructured Fe_2O_3 and CuO composite electrodes for Li ion batteries synthesized and deposited in one step 196 (2011) 6425-6432.
[53] P. Jannacsh, Ionic conducting electrolytes based on aggregating comblike poly(propylene oxide) Polymer 42 (2001) 8629-8635.
[54] Z. Zhang, S. Fang, Ionic conductivity and physical stability study of gel network polymer electrolytes, J. Appl. Polym. Sci. 77 (2000) 2957-2962.
[55] A. J. Blake, N. R. Champness, P. Hubberstery, W. S. Li, M. A. Withersby, M. Schroder, Inorganic crystal engineering using self-assembly of tailored building-blocks, Coordin. Chem. Rev. 183 (1999) 117-138.
[56] H. Aghabozrg, F. Manteghi, S. Sheshmani, A brief review on structural concepts of novel supramolecular proton transfer compounds and their metal complexes, J. Iran. Chem. Soc. 5 (2008) 184-227.
[57] A. Harada, Y. Takashima, H. Yamaguchi, Cyclodextrin-based supramolecular polymers, Chem. Soc. Rev. 38 (2009) 875-882.
[58] A. Harada, Polyrotaxanes, Acta. Polym. 49 (1998) 3-17.
[59] L. Szente, J. Szejtli, Highly soluble cyclodextrin derivatives: chemistry, properties, and trends in development, Adv. Drug. Deliv. Rev. 36 (1999) 17-28.
[60] Y. Okumura, K. Ito, The polyrotaxane gel: a topological gel by figure-of eight cross-links, Adv. Mater. 13 (2001) 485-487.
[61] A. Harada, M. Kamachi, Complex formation between poly(ethylene glycol) and α-cyclodextrin, Macromolecules 23 (1990) 2821-2823.
[62] A. Harada, J. Li, M. Kamachi, The molecular necklace: a rotaxane containing many threaded α-cyclodextrine, Nature 356 (1992) 325-327.
[63] A. Harada, J. Li, M. Kamachi, Preparation and characterization of a polyrotaxane consisting of monodisperse poly(ethylene glycol) and .alpha.-cyclodextrins, J. Am. Chem. Soc. 116 (1994) 3192-3196.
[64]K. Ito, Novel cross-linking concept of polymer network: synthesis, structure, and properties of slide-ring gels with freely movable junctions, Polym. J. 39 (2007) 488-499.
[65] J. Araki, K. Ito, Recent advances in the preparation of cyclodextrin-based polyrotaxanes and their applications to soft materials, Soft Matter. 3 (2007) 1456-1473.
[66] T. Karino, Y. Okumura, C. M. Zhao, T. Kataoka, K. Ito, M. Shibayama, SANS studies on deformation mechanism of slide-ring gel, Macromolecules 38 (2005) 6161-6167.

[67] Y. Shinohara, K. Kayashima, Y. Okumura, C. M. Zhao, K. Ito, Y. Amemiya, Small-angle X-ray scattering study of the pully effect of slide-ring gels, Macromolecules 39 (2006) 7386-7391.

Chapter 2

Ion-conductive and Mechanical Properties of Slide-Ring Gels Swollen with Organic Liquid with Lithium Salts

2.1. Introduction

During the past two decades, many researchers have improved the characteristics of lithium ion batteries, such as high voltage, high energy density, and long cycle life. And generally, stretching microporous polymer films infiltrated electrolyte solution (ES), in which the composed of an organic liquid and lithium salt, are used as separator for lithium ion battery.

Polymer matrix typically used polyethylene (PE), polypropylene (PP) and a copolymer of PE and PP [1-6]. Increasing the energy density by allowing a larger amount of ES in the polymer matrix while satisfying high safety requirements has led to the extensive adoption of pseudo-solidified ESs. Explained in chapter 1.2.1, gel polymer electrolytes (GPEs) which are classed as pseudo-solidified ES, have been developed because of these properties such as free from a leakage and high ionic conductivity. Generally, GPEs are prepared by various methods; inducing thixotropy in the ES by the addition of fumed silica [7], cross-linking monomers in a polymer network in the ES [8], and swelling a polymer matrix with ES [9]. Polyethylene oxide (PEO) [10-18], polypropylene oxide (PPO) [19-20], polyacrylonitrile (PAN) [21-29], polymethyl methacrylate (PMMA) [30-35], and polyvinilidene fluoride-hexafluoropropylene (PVdF-HFP) [36-43] are used for GPEs. GPEs based on PEO or PPO, which are prepared from chemically cross-linked random copolymers of EO and PO, have been reported that they have room temperature conductivity more than 10^{-3} S/cm, however, the polymer network hindered the lithium cation transport of the ES [44]. In contrast, GPEs based on PAN, PMMA or PVdF-HFP, which are prepared by physical cross-linking, have micropores containing ES, and they exhibit high ionic conductivity greater than

3.0×10^{-3} S/cm, in addition to good thermal and electrochemical stability [10,19-43].

On the other hand, GPEs containing a large amount of ES lose their mechanical strength, so that typical GPEs are difficult to achieve both high ionic conductivity and sufficient mechanical strength. Therefore, GPEs with both high ionic conductivity and high mechanical strength needed to be investigated for considering the explosive spread of lithium ion battery applications.

In this chapter, we report the use of SR gels to achieve GPEs with both high ionic conductivity and mechanical ductility, in which an index of mechanical strength.

2.2. Experimental

2.2.1. Materials

PR, in which α-CDs are threaded by PEG (M_w = 35,000), was purchased from Advanced Softmaterials Co., Ltd. According to the information provided by the manufacturer, the number of α-CD rings included in a single PR molecule is estimated to be ca. 98 from ^{1}H nuclear magnetic resonance spectroscopy (NMR) measurements, which corresponds to a stoichiometric α-CD to ethylene oxide unit ratio in the inclusion complex of 1:8.1 (inclusion ratio = 24.7%). To prepare methylated polyrotaxane (MePR) [45-48], dehydrated dimethyl sulfoxide (DMSO; Wako Pure Chemical Industries, Ltd.), potassium *t*-butoxide (*t*-BuOK; Sigma-Aldrich Co.) in tetrahydrofuran (THF), and iodomethane (Tokyo Chemical Industry Co., Ltd.) were used without further purification. Divinyl sulfone (Tokyo Chemical Industry Co., Ltd.) was used as a cross-linker without further purification.

In addition, dehydrated DMSO, dehydrated dimethyl formamide (DMF) and chloroform were used to wash the SR gels. All of these compounds were purchased from Wako Pure Chemical Industries, Ltd. and used without further purification.

A mixture of liquid propylene carbonate (PC; Wako Pure Chemical Industries, Ltd.) and lithium bis(trifluoromethanesulfonyl)imide (LiTFSI; Tokyo Chemical Industry Co., Ltd.) was used as the ES without further purification.

2.2.2. Preparations of MePR

MePRs were prepared with degrees of substitution (DS) at 27.5 and 74.2%. PR (600 mg, 4.61×10^{-6} mol) was dissolved in dehydrated DMSO (24 mL) under a dry N_2 atmosphere and then 1.0 M solutions of *t*-BuOK (1.62 mL for DS of 27.5%; 5.78 mL for DS of 74.2%) was added dropwise, and the dispersion was then stirred for 1 h at room temperature. After the dropwise addition of iodomethane (101 μL (1.62×10^{-3} mol) for DS of 27.4%; 353 μL (5.67×10^{-3} mol) for DS of 74.2%) to the solution, the mixture was stirred overnight at room temperature. This solution was purified by dialysis against deionized water and the solvent was distilled away. DS was calculated from ^{1}H NMR measurements.

^{1}H NMR (δ, ppm in DMSO-d_6): 5.65 [O(2)H of CD], 5.48 [O(3)H of CD], 4.95 [C(1) of CD], 4.47 [O(6)H of CD], 3.8–3.2 [C(2,3,5,6)H of CD], 3.65 (CH_2 of PEG), 3.38 (OCH_3). Figure 2-1 shows NMR spectrums of obtained MePRs.

(a)

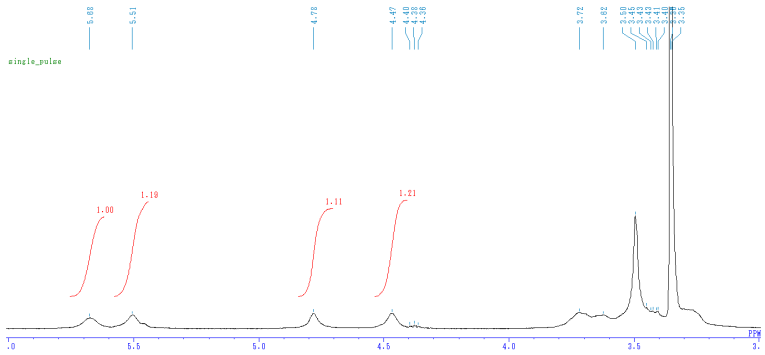

(b)

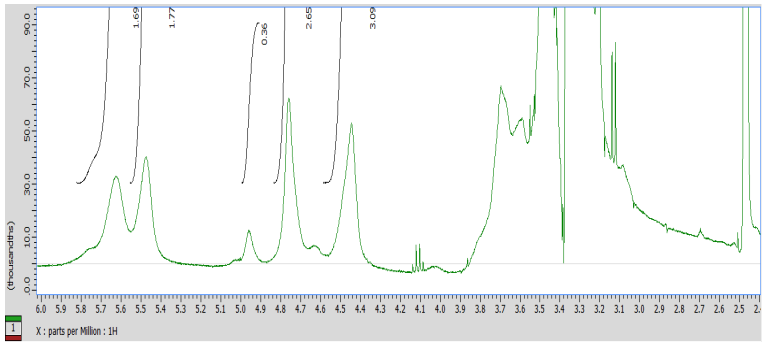

(c)

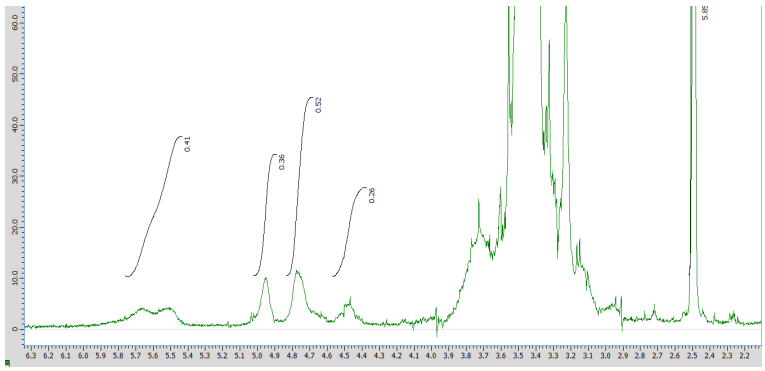

Fig.2-1. NMR spectrums of MePR with DS of (a) 0%. (b) 27.5%. (c) 74.2%.

2.2.3. Preparation of SR gels

PR (50 mg, 5.98×10^{-7} mol) or MePR (50 mg (3.64×10^{-7} mol) for DS of 27.5%; 50 mg (3.36×10^{-7} mol) for DS of 74.2%) was dissolved in 1.0 M NaOH aqueous solution (333 μL), and the solution was settled in a refrigerator for 1 h. Different amounts of divinyl sulfone were added to the solution as a cross-linking reagent. The number ratio of the divinyl sulfone to the hydroxyl group of CD or the sum of the hydroxyl and methyl groups of MeCD (n) was varied from 6.0 to 10.0%. After vortex mixing for 30 min and degassing under vacuum, the samples were settled for 24 h in a refrigerator to obtain PR- or MePR-SR gels. The SR gels were immersed in deionized water, dehydrated DMSO, dehydrated DMF and chloroform, each for 3 h three times to remove any residual impurities and solvent, and then dried in a vacuum chamber overnight. Finally, the dried SR gels were swollen in PC and the ES of 1.0 M LiTFSI (5.74 g) in PC (20.0 mL) for 4 days in a glovebox under a dry N_2 atmosphere to achieve equilibrium swelling (Scheme 2-1).

(a)

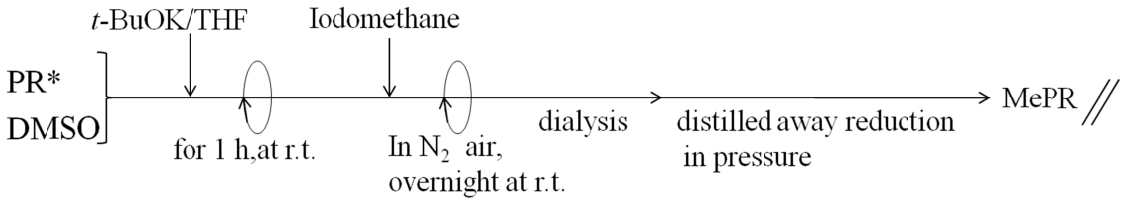

(b)

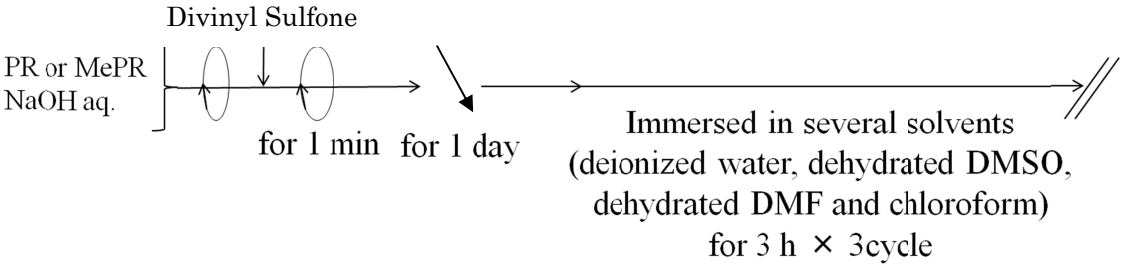

(c)

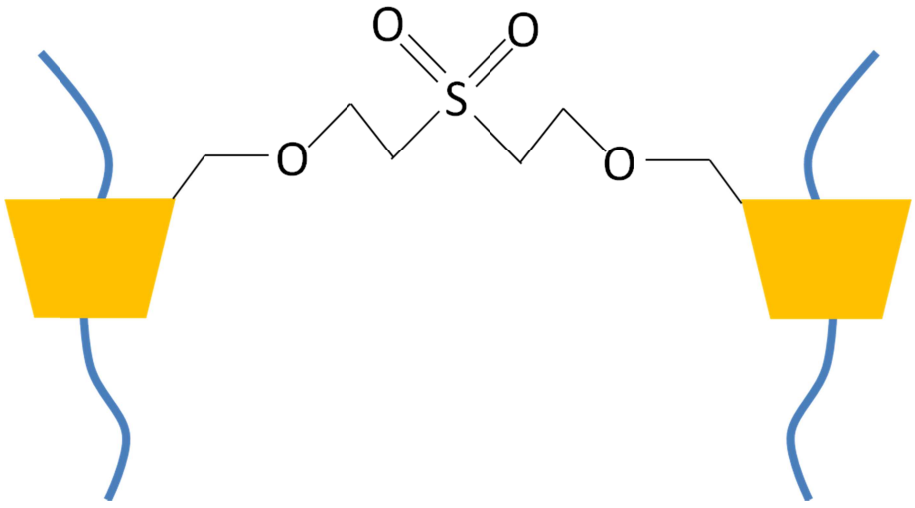

Scheme 2-1. (a) The synthesis of MePR. (b) The synthesis of SR gel. (c) The structure of cross-links between CDs.

PR- and MePR-SR gels prepared with various amounts of cross-linking reagent (different DS and different cross-linking density) were swollen by the ES the ionic conductivity was measured. MePR-SR gels with DS of 74.2%, which were prepared with various amounts of cross-linking reagent and swollen with ES, were used for potential window and compressive measurements.

The weight-swelling ratio Q_w, is defined as $Q_w = W/W_0$, where W_0 is the weight of the dried gel before swelling with PC or ES, and W is the weight of gel after swelling with PC or ES. The volume swelling ratio Q_v, is defined as $Q_v = (L/L_0)^3$, where L_0 is the edge length of the dried gel before swelling with PC or ES, and L is the length of the gel after swelling, assuming that the swelling occurs isotropically. All measurements were performed in a glovebox under a dry N_2 atmosphere.

2.2.4. Electrical measurement

AC impedance measurements were performed to investigate the ionic conductivity of the SR gels swollen with the ES. The gel was cut to have a thickness of 5.00×10^2 μm and an area of 0.282 cm^2, and was sandwiched with a Teflon® spacer between two stainless-steel plates held together with a clip. The AC impedance measurement was performed using a potentiostat/galvanostat meter (SP-150, Bio-Logic, Inc.) within the frequency region of 10^2–10^5 Hz in a glovebox under a dry Ar atmosphere from 293 to 373 K in increments of 10 K.

DC polarization measurements were conducted to investigate the potential window of the SR gels swollen with ES. The gel was cut to a thickness of 5.00×10^2 μm with an area of 0.282 cm^2 and was also sandwiched with a Teflon® spacer between two stainless-steel plates held together with a clip. MePR-SR gels with DS

of 74.2% were prepared with various amounts of cross-linking reagent and swollen with the ES. DC polarization measurements were performed using an impedance analyzer (1280C, Solartron Analytical, AMTEK, Inc.) within the voltage range of 0–6 V with a scan rate of 5 mV/s in a glovebox under a dry Ar atmosphere at 293 K.

2.2.5. Mechanical measurement

Stress-strain measurements were conducted using compaction tests to investigate the mechanical characteristics of the SR gels swollen with ES. MePR-SR gels with DS of 74.2% were prepared with various amounts of cross-linking reagent and swollen with the ES. The stress-strain measurement was performed by a universal tensile testing machine (Tensilon RTC-1250, Orientec Co., Ltd.) in air at room temperature.

2.3. Results and discussion

2.3.1. Swelling behavior of SR gels containing ES

Table 2-1 shows estimated Q_w, Q_v and the volume fraction occupied by PR (φ_v) in the PR- and MePR-SR gel swollen with pure PC or ES in equilibrium. Each gel with different number ratio n of the cross-linking reagent to the hydroxyl group of CD or the sum of the hydroxyl and methyl groups of MeCD was prepared. A pure PC could hardly make the SR gel swell both for PR-SR gel (PR-gel **1-5**) and MePR-SR gel with DS of 27.5 % (MePR-gel **1-5**), while MePR-SR gels with DS of 74.2 % (MePR-gel **6-10**) could be slightly swollen with pure PC. Since PEG, which is

component of PR, can be soluble in PC, the ability of swelling depends on the affinity of PC to CDs or MeCDs. Increasing DS of MeCDs make MePR soluble to pure PC, and consequently MePR-SR gels with DS of 74.2 % was slightly swollen with pure PC. Next, ES, which was 1.0 M PC solution of LiTFSI, could not make PR-SR gel (PR-gel **1-5**) swell at all, while MePR-SR gels (MePR-gel **1-10**) could be swollen with ES very well. This result suggested that solvation effect to PC by forming lithium cation complexes with the ether oxygen atoms onto MeCD caused a large swelling, but lithium cation did not give sufficient affinity of PC and PR in the case of PR-SR gel. As compared to the gels with different DS, the gels with DS of 74.2 %(MePR-gel **6-10**) can be swollen more largely than that with DS of 27.5 % (MePR-gel **1-5**). This result was consistent with above suggestion. On the other hand, PEG can form coordination bonds with lithium ions, so it was suggested that the conformation of the PEG between cross-links was slightly bended by forming the complexes between PEG and lithium ion. Hence, it was suggested that the length between cross-links decreased from that without forming any complex.

Moreover, with decreasing *n*, swelling ratio almost increased at MePR-SR gel swollen by ES. This tendency was common behavior in general gels and was explained that a polymer chain can extend freely by decreasing cross-linking density.

In addition, we describe qualitative properties and appearances of MePR-SR gels swollen with each solvent. The MePR-SR gel with DS of 27.5 % swollen with PC was white opaque. The MePR-SR gels with DS of 74.2 % swollen with PC, deionized water, dehydrated DMSO, dehydrated DMF and chloroform were colorless transparent. Furthermore, the MePR-SR gel with DS of 74.2 %

swollen with chloroform has adhesiveness against glass.

Table 2-1. Weight (Q_w) and volume (Q_v) swelling ratios, and volume fraction (φ_v) of PR-SR and MePR-SR gels immersed in ES pure PC as solvents for equilibrium swelling with various number ratios of the cross-linking reagent, n.

	n / %	No.	Q_w of PC	Q_v of PC	Q_w of ES	Q_v of ES	φ_v / %
PR-SR gel	10	PR-gel **1**	1.0	1.0	1.5	1.5	–
	9.0	PR-gel **2**	1.0	1.0	1.6	1.1	–
	8.0	PR-gel **3**	1.0	1.0	1.2	1.1	–
	7.0	PR-gel **4**	1.0	1.0	1.1	1.0	–
	6.0	PR-gel **5**	1.0	1.0	1.1	1.0	–
MePR-SR	10	MePR-gel **1**	1.0	1.0	13.3	13.5	7.41
gel with DS	9.0	MePR-gel **2**	1.0	1.0	19.5	13.1	7.61
of 27.5 %	8.0	MePR-gel **3**	1.0	1.0	17.3	13.5	7.41
	7.0	MePR-gel **4**	1.0	1.0	20.1	14.4	6.93
	6.0	MePR-gel **5**	1.0	1.0	24.4	14.0	7.14
MePR-SR	10	MePR-gel **6**	3.7	2.7	22.8	12.0	8.31
gel with DS	9.0	MePR-gel **7**	3.9	3.2	21.3	17.6	5.68
of 74.2 %	8.0	MePR-gel **8**	4.1	3.8	27.7	14.0	7.14
	7.0	MePR-gel **9**	4.3	4.6	35.4	14.4	6.93
	6.0	MePR-gel **10**	4.0	5.1	36.8	19.9	5.02

2.3.2. Electrical measurement of SR gels containing ES by equilibrium swelling

AC impedance of PR-SR gel **1**, MePR-gel **1-4**, and MePR-gel **6-10** containing ES was measured. The Arrhenius plot of ionic conductivity of PR-SR gel **1**, MePR-gel **1-4**, and MePR-gel **6-10** containing ES are shown in Fig. 2-1(a), (b) and (c), respectively. Since the SR gel contained the PR network, which did not contribute to the ionic conduction, with a volume fraction of φ_v, σ was under underestimated for the ionic conduction of ES in the SR gel. Hence, the molar conductivity Λ was adopted as the following relation,

$$\Lambda = \sigma/\{c_0(1-\varphi_v)\}, \qquad (1)$$

where c_0 was the concentration of pristine ES (1.00×10^{-3} mol cm^{-3}).

Table 2-2 shows σ, Λ, activation energy ΔE_a and the molar conductivity ratio of Λ to the molar conductivity of pristine ES, $\Lambda_0 = 4.26$ S cm^2 mol^{-1} [11], of PR- and MePR-SR gel with changing n. ΔE_a was calculated from a slope in Fig. 2-1. At first, σ, Λ of PR-SR gel **1** was quite small, because the gel was scarcely swollen even by using ES. From the results of MePR-gel, it was found that the molar conductivities are increasing with DS. This result was due to increasing swelling ratio with increasing DS.

Since Λ was smaller than Λ_0 and decreased with increasing n, it confirmed that polymer matrix disturbed the ionic transport of ES, and this result was consistent with previous report that ionic interaction between PEG and lithium cation disturbed lithium cation transport [49]. Although hydrodynamic radius of lithium cation is enough smaller than the mesh size of SR gel, the interaction between MePR-SR gel network and adjacent PC molecules increases the adjacent

viscosity, hence a macroscopic viscosity that lithium cation suffered from also increases through the hydrodynamic interaction. Then the ionic transport is suggested to be disturbed by this increased viscosity.

However, Λ/Λ_0 was more than 95 % in MePR-gel **10** and its activation energy was 6.42 kJ mol^{-1} [11], which was quite close to that of pristine ES of 6.40 kJ mol^{-1}, hence it was concluded that this gel electrolyte had comparable properties to pristine ES.

(a)

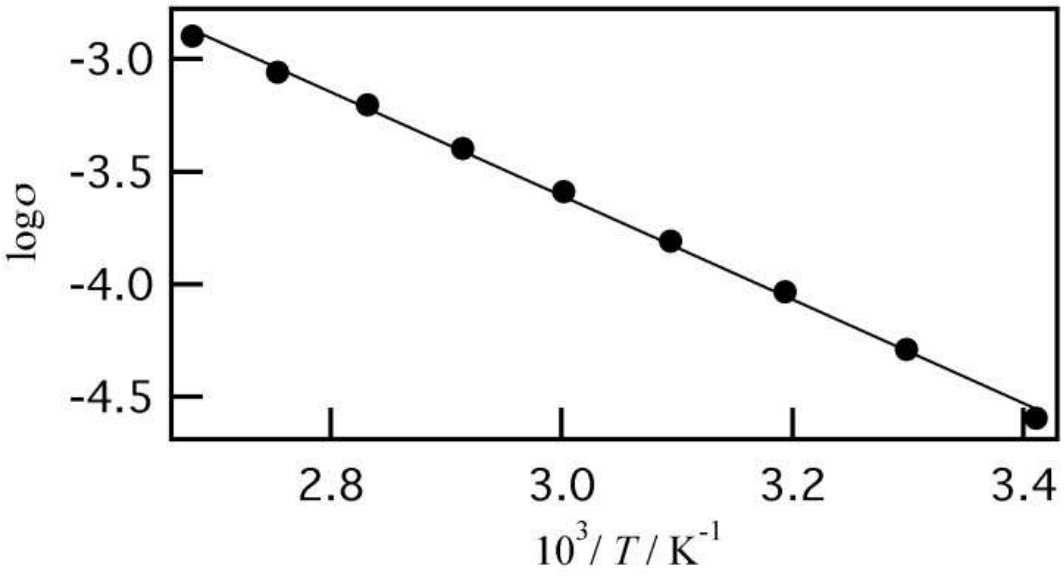

(b)

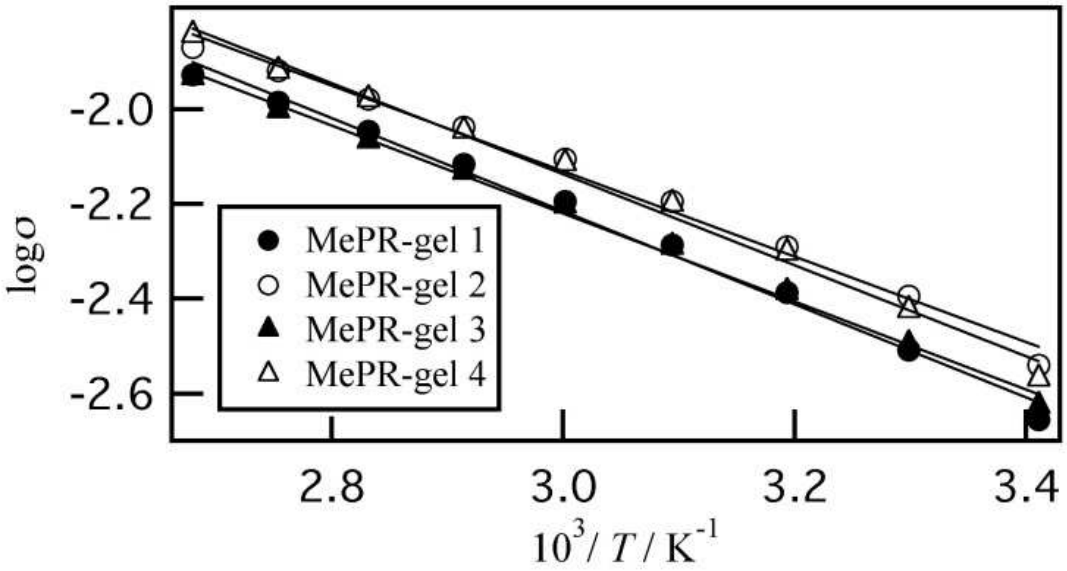

(c)

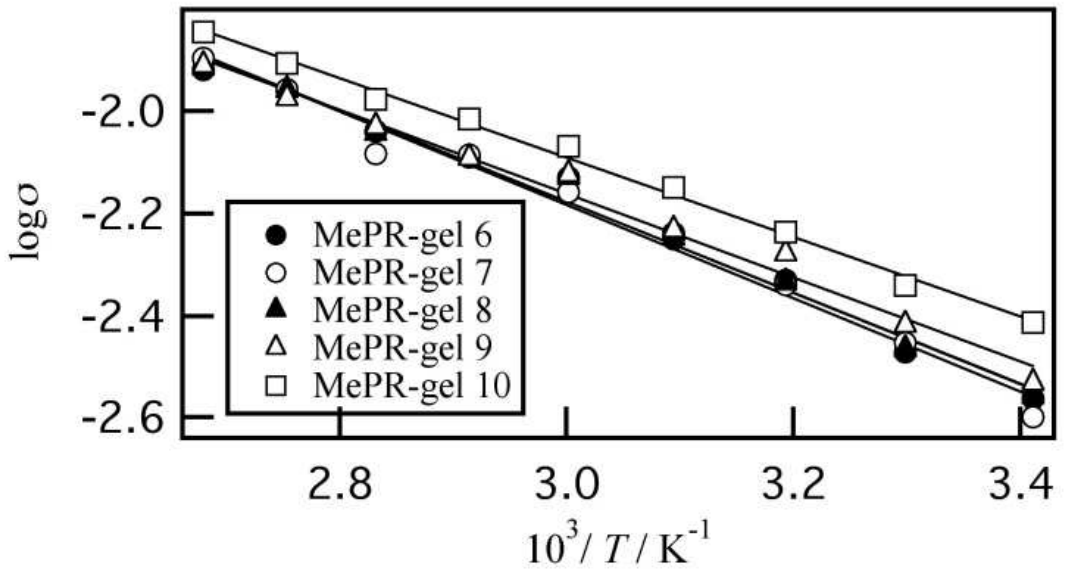

Fig. 2-1. (a) An Arrhenius plot of the ionic conductivity of the PR-gel **1** (●). (b) MePR-gel **1** (●), MePR-gel **2** (○), MePR-gel **3** (▲), MePR-gel **4** (△). (c) MePR-gel **6** (●), MePR-gel **7** (○), MePR-gel **8** (▲), MePR-gel **9** (△), MePR-gel **10** (□).

Table 2-2. Conductivity σ, molar conductivity Λ, the ratio of Λ to the molar conductivity of pristine ES (Λ_0) of the SR gel swollen by ES in equilibrium with changing number ratio of the cross-linking reagent n at 293K, and activation energy ΔE_a estimated from the slope of the temperature dependence.

	No.	σ / mS cm^{-1}	Λ / S cm^2 mol^{-1}	Λ/Λ_0 / %	ΔE_a / kJ mol^{-1}
PR-SR gel	PR-gel **1**	2.54×10^{-5}	1.10×10^{-1}	2.58	19.1
MePR-SR gel with DS of 27.5 %	MePR-gel **1**	2.21	2.38	55.9	8.16
	MePR-gel **2**	2.88	3.12	73.2	7.4
	MePR-gel **3**	2.36	2.55	59.8	7.73
	MePR-gel **4**	2.69	2.89	67.8	7.99
MePR-SR gel with DS of 74.2 %	MePR-gel **6**	2.77	3.02	70.9	7.39
	MePR-gel **7**	2.53	2.68	62.9	7.55
	MePR-gel **8**	2.77	2.98	70.0	7.37
	MePR-gel **9**	2.94	3.16	74.2	6.79
	MePR-gel **10**	3.87	4.07	95.5	6.42

Potential window of MePR-SR gels with DS with of 74.2 % in equilibrium swelling with changing number ratio of cross-linking reagent 4 to 10 % at 293 K are shown in Fig. 2-2. From the results, large number ratio of cross-linking reagent, potential windows were identically 5.5 V, which agreed with the value previously reported on PC-LiTFSI [50]. However, the gels with small cross-linking density showed the increase in the intensity of current at approximately 3.3 V, suggesting that this result be owing to the decomposition of ES. This result suggested that SR gels do not affect potential window. And figure 2-3 shows picture of the gel after potential window measurement.

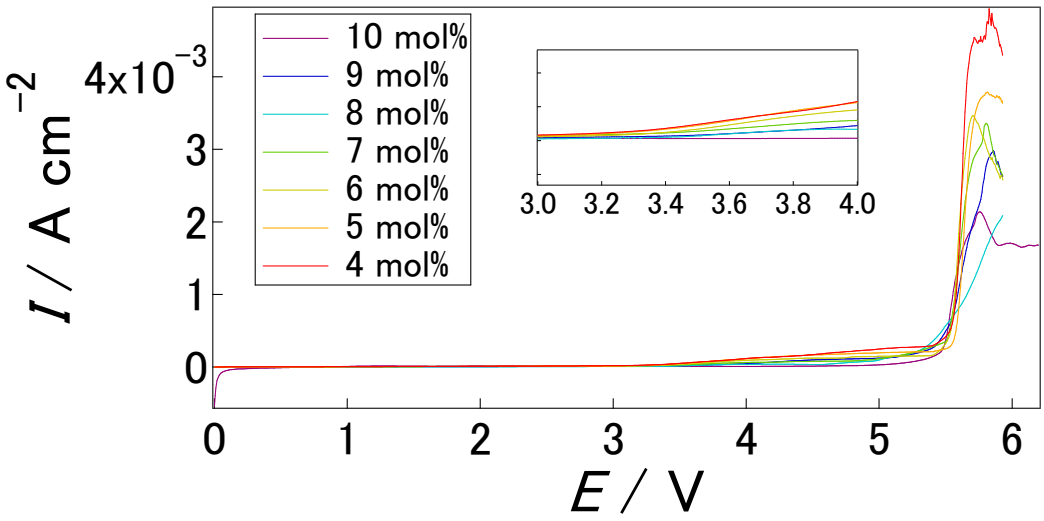

Fig. 2-2. The potential window of MePR-SR gels with DS of 74.2 % in equilibrium swelling with changing number ratio of the cross-linking reagent at 293 K. The inset shows an expanded view of the voltage region from 3.0 to 4.0 V.

Fig. 2-3. The picture of the gel after potential window measurement.

2.3.3. Mechanical properties of swollen MePR-SR gels containing ES

It was known that polymer gel electrolytes containing a large quantity of ES were mechanically brittle [51-52]. However, SR gels have unique structure and are expected to have high ductility. Hence, we measured mechanical property of SR

gel containing a large quantity of ES by compressive test. The stress-strain (S-S) curves of MePR-SR gel **6** - **9** are shown in Fig. 2-4 and photographs of gels after compressed are shown Fig. 2-5(a), (b), (c) and (d). Inicidentally, MePR-SR gel **10** was too soft to be measured. Young's modulus E of MePR-SR gel was calculated from the initial slope and estimated values were shown in Table 2-3. In all gels, E was quite small that meant that these gels were quite soft. In the previous study, E of the polymer gel electrolyte based on PVdF was 1.0 MPa [53] and that of the polymer gel electrolyte based on PVC-PEO was 0.5-2.0 MPa [54], and hence MePR-SR gels were incomparably soft. However, the characteristic feature of SR-gel electrolytes was to disperse effectively the stress and showed the large and reversible ductility, so it is difficult to evaluate the SR-gel electrolyte by an identical benchmark of conventional electrolytes separators. With swelling ratio, that is, decreasing n, E decreased and gel became a bit soft.

As shown in Fig. 2-4, MePR-SR gel **6** was fractured at $\varepsilon = 0.85$, which was not observed obviously in S-S curve, and MePR-SR gel **7** was fractured at $\varepsilon = 0.44$, which was out of region shown in Fig. 2-4, while MePR-SR gel **8** and MePR-SR gel **9** did not fractured under the compression of almost half thickness than its original thickness. Although the fracture point varied by samples, there was a tendency that gels with a small cross-linking density were not fractured under high compression such as $\varepsilon = 0.5$. Since MePR-SR gel **6** and **7** have larger cross-linking density, a minuscule crack of gels may be generated by compression and the crack spread out gradually under high compression. This result suggested that gels with a small cross-linking density were very soft, hence the stress was dispersed and cracks were difficult to generate, so gels were not fractured under high compression. From the

viewpoint of this study, MePR-SR gel **9**, which was methylated SR gel with large DS of 74.2 % and had low cross-linking density of n = 7 %, showed compatible properties, large ionic conductivity more than 95 % of pristine ES and high tolerance against the compression of ε = 0.5. Moreover, plastic deformations were not observed from these S-S curves. In the previous study, reported plastic deformation of gelatin gel was at approximately ε =0.7 [55] and that of epoxy resin was observed at approximately ε =0.9 [56] and that of epoxy resin was observed at approximately ε =0.9 [57]. hence, these SR gel was suggested to be having sufficient toughness. Furthermore, E of the SR gels swollen with other liquid in which water, DMSO and 1-ethyl-3-methylimidazolium chloride, were reported and the values were 650 kPa, 64 kPa and 71 kPa [57], respectively. So, the SR gel swollen with ES suggested soft one.

Table 2-3. Volume swelling ratio with ES, Q_v, E, compression ratio and fracture point.

No.	n / %	Q_v	E / kPa	Compression ratio / %	Fracture point / mm
MePR-gel **6**	10	13.5	20.1	72.3	0.06, 0.48
MePR-gel **7**	9	13.1	19.1	39.3	1.74
MePR-gel **8**	8	14.2	16.9	46.4	—
MePR-gel **9**	7	14.4	14.8	51.5	—

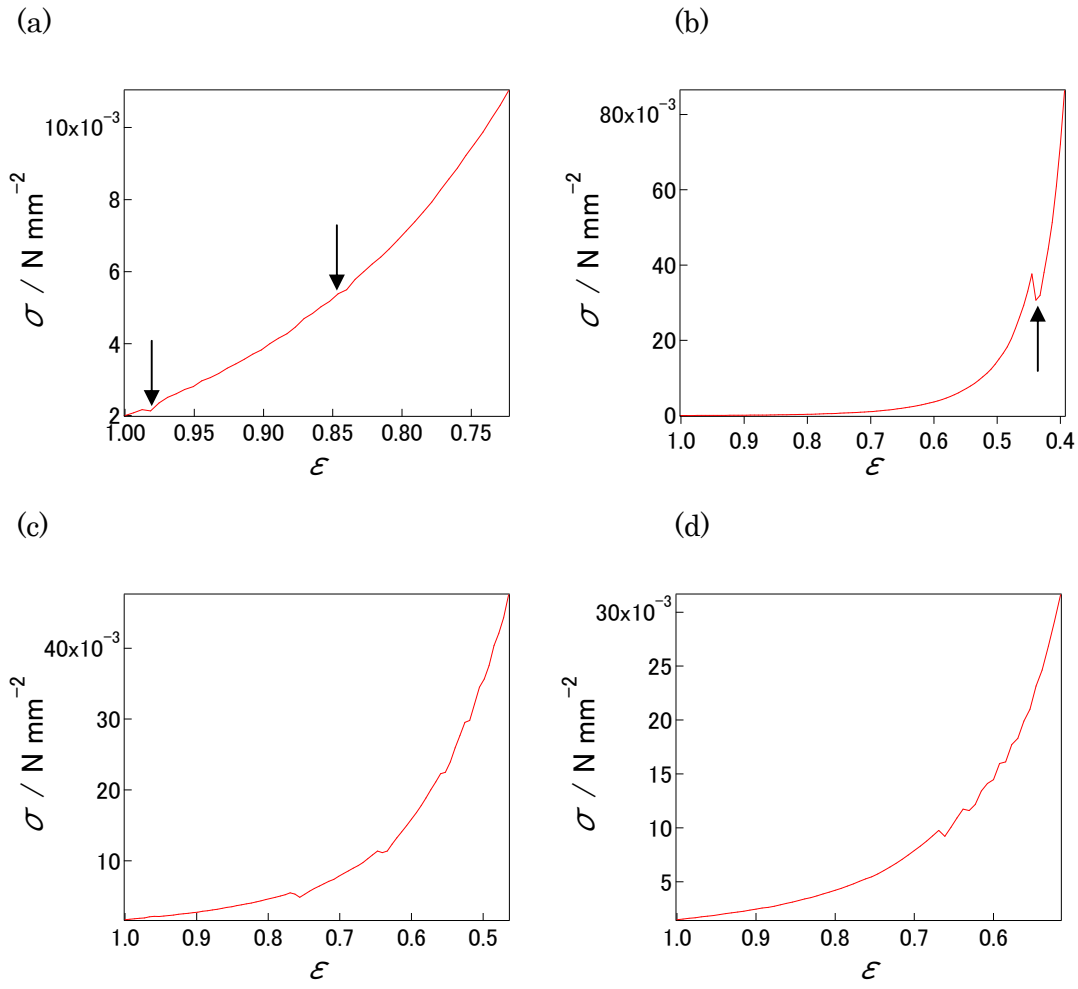

Fig. 2-4. The compressive properties of (a) MePR-gel **6**. (b) MePR-gel **7**. (c) MePR-gel **8**. (d) MePR-gel **9**. And the arrow line means fracture point.

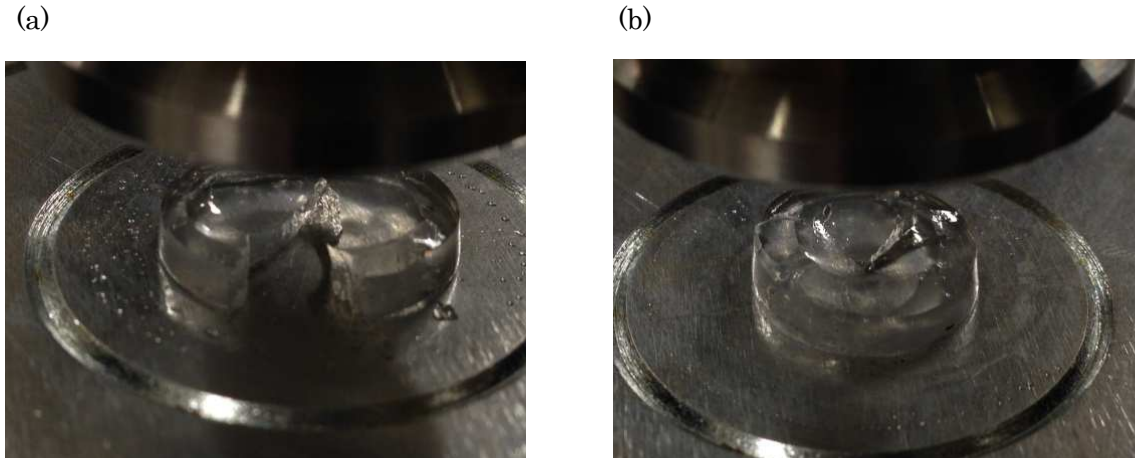

(c)

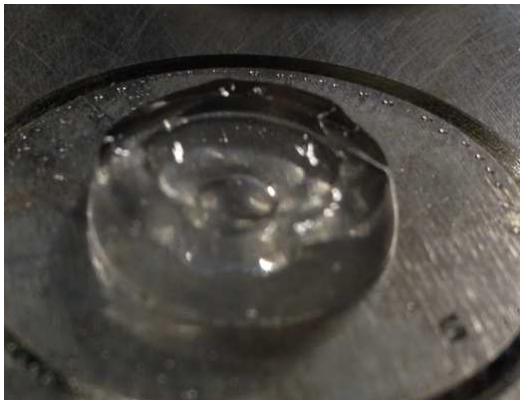

Fig. 2-5. Picture of gels after compressed for (a) MePR-gel **6**. (b) MePR-gel **7**. (c) MePR-gel **9**.

2.4. Summary

The molar conductivity of SR gel (methylated PR with DS of 74.2 %) swollen with ES with high swelling ratio of Q_w more than 30 was more than 95 % of that of pristine ES. The activation energy and potential window of SR gel swollen ES was similar to that of pristine ES. Moreover, the SR gel swollen ES with high swelling ratio and small cross-linking density had small E and was not fractured under the compression of $\varepsilon = 0.85$. In these gels, the stress was dispersed and cracks were difficult to generate, so gels were not fractured under high compression. We achieved the SR gel electrolytes with compatible properties of large ionic conductivity more than 95 % of pristine ES and high tolerance against the compression of $\varepsilon = 0.5$.

References

[1] H. S. Bierenbaum, R. B. Issacson, M. L. Druin, S. G. Plovan, Microporous polymeric films, Ind. Eng. Chem. Prod. Res. Dev., 13 (1974) 2-9.

[2] C. R. Jarvis, W. J. Macklin, A. J. Macklin, N. J. Mattingley, E. Karonfli, Use of grated PVdf-based polymers in lithium batteries, J. Power Sources 97-98 (2001) 664-666.

[3] Y. M. Lee, J. W. Kim, N. S. Choi, J. A. Lee, W. H. Seol, J. K. Park, Novel porous separator based on PVdF and PE non-woven matrix for rechargeable lithium batteries, J. Power Sources 139 (2005) 235-241.

[4] Z. Jiang, B. Carroll, K. M. Abraham, Studies of some poly(vinylidene fluoride) electrolytes, Electrochim. Acta 42 (1997) 2667-2677,

[5] S. S Choi, Y. S. Lee, C. W. Joo, S. G. Lee, J. K. Park, K. S. Han, Electrospun PVDF nanofiber web as polymer electrolyte or separator, Electrochim. Acta 50 (2004) 339-343.

[6] M. Armand, The history of polymer electrolytes, Sol. St. Ion. 69 (2002) 309-319.

[7] V. Gentili, S. Panero, P. Reale, B. Scrosati, Composite gel-type polymer electrolyte for advanced, rechargeable lithium batteries, J. Pow. Sources 170 (2007) 185-190.

[8] K. M. Abraham, M. Alamgir, D. K. Hoffman, Polymer electrolytes reinforced by celgard® membranes, J. Electrochem. Soc. 142 (1995) 683-687.

[9] P. P. Prosini, S. Passerini, A lithium battery electrolyte besed on gelled polyethylene oxide, Sol. St. Ion. 146 (2002) 65-72.

[10] C. S. Kim, S. M. Oh, Importance of donor number in determining solvating ability of polymers and transport properties in gel-type polymer electrolytes, Electrochim. Acta 45 (2000) 2101-2109.

[11] Y. Aihara, S. Arai, K. Hayamizu, Ionic conductivity, DSC and self diffusion coefficients of lithium, anion, polymer, and solvent of polymer gel electrolytes: the structure of the gels and the diffusion mechanism of the ions, Electrochim. Acta 45 (2000) 1321-1326.

[12] E. M. Cha, D. R. Macfarlane, M. Forsyth, C. W. Lee, Ionic conductivity studies of polymeric electrolytes containing lithium salt with plasticizer, Electrochim. Acta 50 (2004,) 335-338.

[13] C. P. Tien, H. S. Teng, Effocoent ion transport in activated carbon capacitors assembled with gelled polymer electrolytes based on poly(ethylene oxide) cured with poly(propylene oxide) diamines, J. Taiwan Inst. Chem. Eng. 40 (2009) 452-456.

[14] Z. Y. Cui, Y. Y. Xu, L.P. Zhu, J. Y. Wang, Z. Y. Xi, B. K. Zhu, Preparation of PVDF/PEO-PPO-PEO blend microporous membranes for lithium ion batteries via thermally induced phase separation, J. Membr. Sci. 325 (2008) 957-963.

[15] P. Jannasch, Ion conducting electrolytes based on aggregating comblike

poly(propylene oxide), Polymer 42 (2001) 8629-8635.
[16] V. D. Nato, M. Vittadello, K. Yoshida, S. Lavina, E. Negro, T. Furukawa, Broadband dielectric and conductivity spectroscopy of Li-ion conducting three-dimensional hybrid inorganic-organic networks as polymer electrolytes based on poly(ethylene glycol) 400, Zr and Al nodes, Electrochim. Acta 57 (2011) 192-200.
[17] V. Di. Noto, V. Zago, Inorganic-organic polymer electrolytes based on PEG400 and Al[OCH(CH3)2]3 1. Synthesis and vibrational characterizations, J. Electrochem. Soc. 151, (2004) A216-A223.
[18] V. Di. Noto, V. Zago, Inorganic-organic polymer electrolytes based on PEG400 and Al[OCH(CH3)2]3 2. Morphology, thermal stability, and conductivity mechanism, J. Electrochem. Soc. 151, (2004) A224-A231.
[19] Z. Y. Cui, Y. Y. Xu, L.P. Zhu, J. Y. Wang, Z. Y. Xi, B. K. Zhu, Preparation of PVDF/PEO-PPO-PEO blend microporous membranes for lithium ion batteries via thermally induced phase separation, J. Membr. Sci. 325 (2008) 957-963.
[20] P. Jannasch, Ion conducting electrolytes based on aggregating comblike poly(propylene oxide), Polymer 42 (2001) 8629-8635.
[21] M. Watanabe, M. Kanba, K. Nagaoka, I. Shinohara, Ionic conductivity of hybrid films based on polyacrylonitrile and their battery application, J. Appl. Polym. Sci. 27 (1982) 4191-4198.
[22] K. M. Abraham, M. Alamgir, Li^+-conductive solid polymer electrolytes with liquid-like conductivity, J. Electrochem. Soc. 137 (1990) 1657-1658.
[23] H. Akashi, K. Sekai, K. Tanaka, A novel fire-retardant polyacrylonitrile –based gel electrolyte for lithium batteries, Electrochem. Acta 43 (1998) 1193-1197.
[24] S. Slane, M. Salomon, Composite gel electrolyte for rechargeable lithium batteries, J. Pow. Sources 55 (1995) 7-10.
[25] H.R. Jung, D. H. Ju, W. J. Lee, X. W. Zhang, R. Kotek, Electrospun hydrophilic fumed silica/polyacrylonitrile nanofiber-based composite electrolyte membranes, Electrochim. Acta 54(2009) 3630-3637.
[26] A. I. Gopalan, P. Santhosh, K. M. Manesh, J. H. Nho, S. H. Kim, C. G. Hwang, K. P. Lee, Development of electrospun PVdF-PAN membrane-based polymer electrolytes for lithium batteries, J. Membr. Sci. 325 (2008) 683-690.
[27] B. Y. Huang, Z. X. Wang, L. Q. Chen, R. J. Xue, F. S. Wang, The mechanism of lithium ion transport in polyacrylonitrile-based polymer electrolytes, Sol. St. Ion. 91 (1996) 279-284.
[28] T. Osaka, T. Momma, H. Ito, B. Scrosati, Performances of lithium/gel electrolyte/polypyrrole secondary batteries, J. Pow. Sources 68 (1997) 392-396.

[29] S. Mitra, A. K. Shukla, S. Sampath, Electrochemical capacitors with plasticized gel-polymer electrolytes, J. Pow. Sources 101 (2001) 213-218.
[30] O. Bohnke, M. Frand, M. Rezrazi, C. Rousselot, C. Truche, Fast ion transport in new lithium electrolytes gelled with PMMA. 2. influence of polymer concentration, Sol. St. Ion. 66 (1993) 105-112.
[31] P. E. Stallworth, S. G. Greenbaum, F. Croce, S. Slane, M. Salomon, Lithium-7 NMR and ionic conductivity studies of gel electrolytes based on poly(methylmethacrylate), Electrochim, Acta 40 (1995) 2137-2141.
[32] F. Croce, S. D. Brown, S. G. Greenbaum, S. M. Slane, M. Salomon, Lithium-7 NMR and ionic conductivity studies of gel electrolytes based on polyacrylonitrile, Chem. Mater. 5 (1993) 1268-1272.
[33] J. Vondrak, M. Sedlarikova, J. Velicka, B. Klapste, V. Novak, J. Reiter, Gel polymer electrolytes based on PMMA, Electrochim. Acta 46 (2001) 2047-2048.
[34] H. P. Zhang, P. Zhang, Z. H. Li, M. Sun, Y. P. Wu, H. Q. Wu, A novel sandwiched membrane as polymer electrolyte for lithium ion battery, Electrochem. Commun. 9 (2007) 1700-1703.
[35] S. Rajendran, T. Uma, Lithium ion conduction in PVC-$LiBF_4$ electrolytes gelled with PMMA, J. Pow. Sources 88 (2000) 282-285.
[36] C. Capiglia, Y. Saito, H. Kataoka, T. Kodama, E. Quartarone, P. Mustarelli, Structure and transport properties of polymer gel electrolytes based on PVdF-HFP and$Li(C_2F_5SO_2)_2$, Sol. St. Ion. 131 (2001) 291-299.
[37] A. M. Stephan, S. G. Kumar, N. G. Renganathan, M. A. Kulandainathan, Characterization of poly(vinylidene fluoride-hexafluoroprplylene) (PVdF-HFP) electrolytes complexed withdifferent lithium salts, Eur. Polym. J. 41 (2005) 15-21.
[38] A. M. Stephan, K. S. Nahm, M. A. Kulandianathan, G. Ravi, J. Wilson, Poly(vinilidene fluoride-hexafluoropropylene) (PVdF-HFP) based composite electrolytes for lithium batteries, Eur. Polym. J. 42 (2006) 1728-1734.
[39] D. Saika, A. Kumar, Ionic conduction in P(VDF-HFP)/PVDF-(PC+DEC)-$LiCLO_4$ polymer gel electrolytes, Electrochim. Acta 49 (2004) 2581-2589.
[40] H. S. Kim, S. I. Moon, Electrochemical properties of the Li-ion polymer batteries with P(VDF-co-HFP)-based gel polymer electrolyte, J. Pow. Sources 141 (2005) 293-297.
[41] S. Abbrent, J. Plestil, D. Hlavata, J. Lindgren, J. Tegenfeldt, A. Wendsjo, Crystallinity and morphology of PVdF-HFP-based gel electrolytes, Polymer 42 (2001) 1407-1416.
[42] Z. H. Li, G. Y. Su, X. Y. Wang, D. S. Gao, Micro-porous P(VDF-HFP)-based polymer electrolyte filled with Al_2O_3 nanoparticles, Sol. St. Ion. 176 (2005) 1903-1908.

[43] W. H. Pu, X. M. He, L. Wang, C. Y. Jiang, C. R. Wan, Preparation of PVDF-HFP microporous membrane for Li-ion batteries by phase inversion, J. Membr. Sci. 272 (2006) 11-14.
[44] M. Kono, E. Hayashi, M. Nishiura, M. Watanabe, Chemical and Electrochemical Characterization of Polymer Gel Electrolytes Based on a Poly(alkylene oxide) Macromonomer for Application to Lithium Batteries, J. Electrochem. Soc. 147 (2000) 2517-2524.
[45] J. Araki, K. Ito, Polyrotaxane derivatives. 1. Preparation of modified polyrotaxane with nonionic functional groups and their solubility in organic solvents, J. Polym. Sci., Part A: Polym. Chem. 44 (2006) 6312-6323.
[46] M. Kidowaki, C. Zhao, T. Kataoka, K. Ito, Thermorevesible sol-gel transition of aqueous solution of polyrotaxane composed of highly methylated α-cyclodextrin and polyethylene glycol, Chem. Commun. 39 (2006) 4102-4103.
[47] T. Kataoka, M. Kidowaki, C. Zhao, H. Minamikawa, T. Shimizu, K. Ito, Local and network structure of thermoreversible polyrotaxane hydrogels based on poly(ethylene glycol) and methylated α-cyclodextrins, J. Phys. Chem. B 110 (2006) 24377-24383.
[48] T. Karino, Y. Okumura, C. Zhao, M. Kidowaki, T. Kataoka, K. Ito, M. Shibayama, Sol-gel transition of hydrophocally modified polyrotaxane, Macromolecules 39 (2006) 9435-9440.
[49] M. Kono, E. Hayashi, M. Nishiura, M. Watanabe, Chemical and Electrochemical Characterization of Polymer Gel Electrolytes Based on a Poly(alkylene oxide) Macromonomer for Application to Lithium Batteries, J. Electrochem. Soc. 147 (2000) 2517-2524.
[50] K. Kanamura, T. Umegami, S. Shiraisi, M. Ohashi, Z. Takehara, Electrochemical behavior of Al current collector of rechargeable lithium batteries in propylene carbonate with $LiCF_3SO_3$, $Li(CF_3SO_2)_2N$, or $Li(C_4F_9SO_2)(CF_3SO_2)N$, J. Electrochem. Soc. 149 (2002) A185-A194.
[51] Y. Wang, J. Travas-Sejdic, R. Steiner, Polymer gel electrolyte supported with mictroporous polyolefin membranes for lithium ion polymer battery, Sol. St. Ion. 148 (2002) 443-449.
[52] M. Wachtler, D. Ostrovskii, P. Jacobsson, B. Scrosati, A study on PVdF-based SiO_2-containig composite gel-type polymer electrolytes for lithium batteries, Electrochim. Acta 50 (2004) 357-361.
[53] Y. J. Wang, D. Kim, Crystallinity, morphology, mechanical properties and conductivity study of in situ formed PVdF/LiClO4/TiO2 nanocomposite polymer electrolytes, Electrochim. Acta 52 (2007) 3181-3189.

[54] S. Ramesh, T. Winie, A. K. Arof, Investigation of mechanical properties of polyvinyl chloride-polyethylene oxide (PVC-PEO) based polymer electrolytes for lithium polymer cells, Eur. Polym. J., 43 (2007) 1963-1968.
[55] K. Nakamura, E. Shinoda, M. Tokita, The influence of compression velocity on strength and structure for gellan gels, Food Hydeoxolloid 15 (2001) 247-252.
[56] H. Kishi, T. Naitou, S. Matsuda, A. Murakami, Y. Muraji, Y. Nakagawa, Relationships between mechanical properties and nano-structures of DICY-cured epoxy resins, 日本接着学会誌, 41 (2005) 84-92.
[57] S. M. Wally, J. E. Field, Strain rate sensitivity of polymer in compression from low to high rates, Daymat J. 1 (1994) 211-227.
[58] S. Samitsu, J. Araki, T. Kataoka, K. Ito, New solvent for polyrotaxane. II. Dissolution behavior of polyrotaxane in ionic liquids and preparation of ionic liquid-containing slide-ring gels, J. Polym. Sci. Part B 44 (2006) 1985-1994.

Chapter 3

Ionic Conduction in Slide-Ring Gel Swollen with Ionic Liquids

3.1. Introduction

Ionic liquid (IL) is defined as liquid composed of entirely ions that at least one of an anion or a cation must be an organic ion, and having below 100 ℃ melting point [1]. The excellent characteristics of ILs [2-6], such as negligible vapor pressure, non-flammability, high ionic conductivity, and wide electrochemical window, has been attracted to be applied in electrochemical devices such as batteries [7-9], super-capacitors [10-12], and solar cells [13-14]. On the other hand, maintaining these unique properties needs pseudo-solidified ILs from the viewpoint of preventing leakage.

Pseudo-solidified ILs by gelation have been reported using low-molecular weight compounds [14-16], inorganic nanoparticles [13,17] and carbon nanotubes [18-20]. Besides, Watanabe and co-workers have reported pseudo-solidified IL by polymer gels [21-23]. They prepared the polymerized IL with methyl methacrylate (MMA) and common IL, 1-ethyl-3-methylimidazolium bis(trifluoromethane sulfone)imide (EMITFSI), by a cross-linker, and they obtained self-standing, flexible and transparent polymer gels. With a large amount of EMITFSI, the gel of ionic conductivity had a high value of close to 10^{-2} S/cm, which is close to 60 % of that of pure IL, at room temperature and the mechanism of ionic transporting results in the vehicle mechanism rather than the Grotthuss mechanism [23]. In addition, pseudo-solidified ILs with other polymers have also been reported.

In this chapter, we report the conductivity of SR gels containing ILs with various amounts of cross-linking reagents of SR gels, with the intent to clarify the ionic conduction mechanism of ILs in the SR gel network. Furthermore, under the compression, in which the SR gel with elastic deformation without fracturing, the

relation between the polymer network and ionic conduction was investigated.

3.2. Experimental

3.2.1. Materials

Polyrotaxane (PR), in which α-CDs are threaded by PEG (MW = 35,000), and hydroxypropyl polyrotaxane (HyPR), in which ca. 50 % of the hydroxyl group of α-CD of PR was modified by hydroxypropyl group, were obtained from Advanced Softmaterials Co. Ltd. According to information from the supplier, the number of α-CD rings included in the single PR or HyPR was estimated to be ca. 98 by ^{1}H NMR, which corresponds to a stoichiometric ratio of the α-CDs to the EO units in the inclusion complexes of 1:8 (inclusion ratio = 24.7 %). HyPR shows high solubility in water different from PR, because the steric barrier due to the hydroxypropyl group prevents forming hydrogen bonding between two adjacent α-CDs in HyPR. As a cross-linker, we used 1,4-butanediol diglycidil ether purchased from Tokyo Chemical Industry Co., Ltd., without further purification.

Nine kinds of ILs for the swelling gels were used in this study, including 1-ethyl-3-methylimidazolium ethylsulfate (EMIES: **1**), 1-ethyl-3-methylpyridinium ethylsulfate (EMPES: **2**), 1-buthyl-3-methylimidazolium iodide (BMII: **3**), 1-buthyl-3-methylimidazolium chloride (BMICl: **4**), 1-buthyl-3-methylimidazolium bromide (BMIBr: **5**), 1-buthyl-3-methylimidazolium tetrachloroferrate ($BMIFeCl_4$: **6**), 1-buthyl-3-methylimidazolium tetrafluoroborate ($BMIBF_4$: **7**), 1-buthyl-3-methylimidazolium bis(trifluoromethanesulfonyl)imide (BMITFSI: **8**), and 1-ethyl-3-methylimidazolium bis(trifluoromethanesulfonyl)imide (EMITFSI: **9**). All of these compounds were purchased from the Tokyo Chemical Industry Co. Ltd.

and were used without further purification. Cation species of these ILs were alkylimidazolium or alkylpyridinium, and the difference in the swelling property of SR gel containing various ILs was strongly dependent on the anion species of the ILs. The ILs with anion species of ethyl sulfate **1**,**2** and halogen ions ion **3**-**5** with relatively high Lewis basicity were miscible with water, that is, hydrophilic, while ionic liquids with other anion species **6**-**9** with relatively low Lewis basicity were immiscible with water, that is, hydrophobic, and the swelling property of the SR gel was consistent with these affinities.

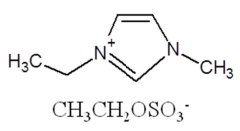 1-ethyl-3-methylimidazolium ethyl sulfate (EMIES: **1**)	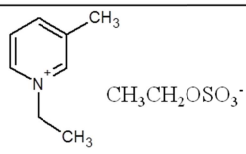 1-ethyl-methyl pyridinium ethyl sulfate (EMPES: **2**)	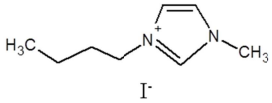 1-butyl-3-methylimidazolium iodide (BMII: **3**)
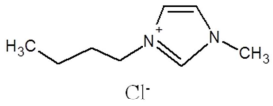 1-buthyl-3-methylimidazolium chloride (BMICl: **4**)	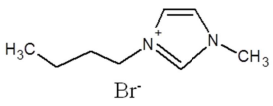 1-buthyl-3-methylimidazolium bromide (BMIBr: **5**)	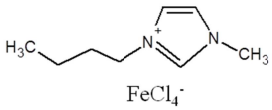 1-buthyl-3-methylimidazolium tetrachloroferrare ($BMIFeCl_4$: **6**)
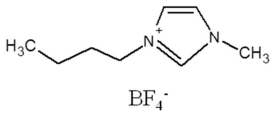 1-buthyl-3-methylimidazolium tetrafuloroborate ($BMIBF_4$: **7**)	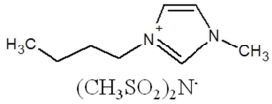 1-buthyl-3-methylimidazolium bis(trifluorosulfonyl)imide (BMITFSI: **8**)	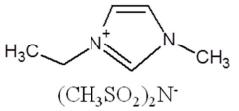 1-ethyl-3-methylimidazolium bis(trifluorosulfonyl)imide (EMITFSI: **9**)

Fig.3-1. Molecular structures of ILs.

3.2.2. Preparations of SR gels

PR (33.0 mg, 2.53×10^{-7} mol) or HyPR (33.0 mg, 1.82×10^{-7} mol) was dissolved in NaOH aqueous solution (1 M) with 14.4 wt%, and then 1,4-butanediol

diglycidyl ether (8.25 μL, 4.37×10^{-5} mol) was added to the solution as a cross-linking reagent by a method reported previously [24]. The number ratio of the cross-linking reagent to the hydroxyl group of the CD or the sum of the hydroxyl and hydroxypropyl groups of HyCD (n) was fixed at 9.8 % in PR and 13 % in HyPR. After several minutes of stirring and degassing in a rough vacuum, the samples were stood still for 24 h at room temperature, and then PR- or HyPR-SR gel was obtained. The SR gels were dipped in Milli-Q water for 5 h three times for removing any residual impurity, and then dried in a vacuum chamber at 80 °C overnight. Finally, the dried SR gels were swollen in ILs **1**-**9** for 7 days at 80 °C as equilibrium swelling, and were clipped to disk-shape with a thickness of 0.3 cm with an area of the base of 0.8 cm^2.

Samples using the IL **1** were prepared by changing the amount of the cross-linking reagent for measuring the ionic conductivity of the SR gels with different cross-linking densities, where n was varied from 6.5 to 52 % (PR-SR gel **1**-**6**), and from 9.1 to 73 % (HyPR-SR gel **1**-**6**). PR-SR gels **1**-**6** and HyPR-SR gels **1**-**6** were swollen in the IL **1** for 7 days at 80 °C as equilibrium swelling, and were clipped out to a disk-shape with a thickness of 0.3 cm and an area of the base of 0.8 cm^2. Gels of n = 6.5 in PR-SR gel and n = 9.1 in Hy-PR gel were so soft that they need to be taken quite carefully.

Further, for measuring the conductivity under compressive deformation, SR gels swollen to less than equilibrium were prepared. n was fixed at 9.8 % (PR-SR gel **7**, HyPR-SR gel **7**) and 13 % (PR-SR gel **8**, HyPR-SR gel **8**), and the dried SR gels were swollen in IL **1** with the mass fraction of PR or HyPR of about 10 wt% by drawing out gels from the IL during swelling at specific times. These were clipped to

a disk shape with a thickness of 0.3 cm and area of the base of 0.8 cm^2.

3.2.3. Synthesis of non-SR gel swollen with IL

Using the method reported by Watanabe and coworkers [23], non-SR gel was prepared by the radical polymerization of a vinyl monomer in IL for comparison with the SR gels under compressive deformation. Methyl methacrylate (MMA) (0.235 g, 2.35×10^{-3} mol) and ethylene glycol dimethacrylate (EGDMA) (9.32 mg, 4.70×10^{-5} mol) were added to IL **9** (1.40 mL) with comparable mass fraction of network polymer to PR gels, and benzoyl peroxide (BPO) (11.4 mg, 4.70×10^{-5} mol) was then added as an initiator. The amount of EGDMA and BPO corresponded to 1.5 mol% (MMA gel **1**) and 2.0 mol% (MMA gel **2**) to the amount of MMA with comparable cross-linking density of network polymer to PR gels. The mixture was poured into a disk-shape Teflon® mold with a thickness of 0.3 cm and area of the base of 0.8 cm^2, and gelated at 80 °C for 24 h to obtain a MMA gel swollen with IL. All of these operations were performed in a nitrogen gas atmosphere.

3.2.4. Characterization of SR gels

The weight swelling ratio Q_w is defined as $Q_w = W / W_0$, where W_0 is the weight of the dried gel before being swollen with ionic liquid, and W the weight of the gel after being swollen with ionic liquid. The volume swelling ratio Q_v is defined as $Q_v = (L / L_0)^3$, where L_0 is an edge length of the dried gel before being swollen with ionic liquid, and L is the edge length of the gel after being swollen with the ionic liquid by assuming that the swelling occurs isotropically. Dynamic elasticity was evaluated with an RSA-II rheometer solids analyzer (TA Instruments Inc.) with a

parallel plate configuration. All measurements were performed in compression mode under air atmosphere within the linear response region with a fixed strain amplitude of 3 % at frequency ranging from 0.1 to 30 Hz at room temperature.

3.2.5. Measurement of ionic conductivity

For investigating ionic conduction of neat IL and SR gels swollen with ILs, AC impedance measurements were performed. The gel was sandwiched between two Pt electrodes sputter-deposited on glass plates separated from each other by a Teflon® spacer with thickness adjusted to the gel samples clipped to a disk shape and the cell was covered with an aluminum foil to remove noises occurred by external electric field. The AC impedance measurement was performed by a ZM2353 impedance meter (NF Circuit Design Block Co., Ltd.) within the frequency region from 10^2 to 2×10^5 Hz in air at room temperature.

Impedance measurements under compressive deformation were performed by clamping the gels sandwiched between Pt electrodes without a Teflon® spacer using an iron vice. The compression ratio λ is defined as $\lambda = t / t_0$, where t_0 is the thickness of the gel before compression, and t is the thickness of the gel after compression.

3.3. Results and discussion

3.3.1. Swelling behavior of SR gels containing IL

The weight swelling ratio Q_w of the PR-SR gel and HyPR-SR gel containing various ILs in equilibrium swelling was estimated as shown in Table 3-1.

Hydrophilic ILs with anion species of ethyl sulfate **1**,**2** and halogen ions **3**-**5** can make the SR gel swell with Q_w of more than 28, while hydrophobic ILs **6**-**9** cannot make the SR gel swell both for PR- and HyPR-SR gel. This tendency was consistent with a previous report on PR-SR gel containing ILs [25], and the difference between PR- and HyPR-SR gel cannot be observed intrinsically. These results of swelling behavior were suggested to be caused by the hydrophilic groups on CDs. Both the hydroxyl groups on CD and hydroxypropyl groups on HyCD are hydrophilic, therefore these PR- and HyPR-SR gels can be swollen with hydrophilic ILs and can be not swollen with hydrophobic ILs. On the other hand, the hydrogen bonding between CDs makes PR insoluble in almost all solvents except for dimethyl sulfoxide (DMSO) and alkaline water, while in HyPR, the hydrogen bonding between CDs is hindered sterically and hence HyPR can be dissolved in some solvents including neutral water. These tendencies are expected to appear in SR gels, but the obvious difference between PR- and HyPR-SR gel containing ILs cannot be observed in the swelling properties including the swelling ratio, which suggested that the affinity of PEG and ILs was dominant in these swelling behaviors. And figure 3-2 shows pictures of the SR gel swollen with IL **1** and **2**.

(a) (b)

Fig.3-2. SR gels swollen with (a)EMIES: **1**. (b) EMIPS: **2**.

Table 3-1. Swelling property, weight swelling ratio Q_w, and IL quantity in wt% of SR gels using various ionic liquids.

Ionic liquids	PR-SR gel			HyPR-SR gel		
	Swelling	Q_w	IL quantity / wt%	Swelling	Q_w	IL quantity /wt%
1	+	33.8	97.1	+	29.6	96.7
2	+	34.8	97.2	+	33.5	97.1
3	+	28.4	96.6	+	30.9	96.9
4	+	31.8	97.0	+	32.1	97.0
5	+	33.6	97.1	+	33.5	97.1
6	–	–	–	–	–	–
7	–	–	–	–	–	–
8	–	–	–	–	–	–
9	–	–	–	–	–	–

Table 3-2 shows estimated Q_w, Q_v, and the volume fraction occupied by PR (φ_v) in the PR-SR gel and HyPR-SR gel containing IL **1** in equilibrium swelling with

changing number ratio *n* of the cross-linking reagent to the hydroxyl group of CD or the sum of the hydroxyl and hydroxypropyl groups of HyCD. Although the ratio of an effective cross-linker to the feeding reagent could not be clarified, the swelling ratio in equilibrium swelling decreased, that is, φ_V increased with *n*, which indicated that the density of the cross-links increased with *n*. Furthermore, compared these results of swelling ratio with that of SR gels swollen with organic liquid including lithium salts, which were measured in section 2.3.2, the SR gels were swollen with IL at larger extent. These results were ascribed to the difference of conformation of PEG chains in equilibrium swelling. In section 2.3.2, we explained the conformation of the PEG was slightly bended by forming the complex by lithium ions. On the other hand, when SR gels swollen with ILs have no lithium ions for forming the complexes in their solutions, PEG between cross-links in these SR gels seemed to be extended, and the swelling ratios of PR- and HyPR-SR gels were approximately close because of using the same PEG, M_W = 35,000, in both PR- and HyPR-SR gels.

Table 3-2. Weight and volume swelling ratio Q_w and Q_v, IL quantity in wt%, and volume fraction φ_v of SR gel in equilibrium swelling by ionic liquid **1** with changing number ratio of the cross-linking reagent *n*.

	No.	*n* / %	Q_w	IL quantity / wt%	Q_v	φ_v / %
PR-SR gel	PR-gel **1**	6.5	50.1	98.0	36.8	2.71
	PR-gel **2**	9.8	33.8	97.1	25.2	3.98
	PR-gel **3**	13	23.9	96.0	16.8	5.95
	PR-gel **4**	26	17.2	94.5	10.9	9.17
	PR-gel **5**	39	10.9	91.6	9.90	10.1
	PR-gel **6**	52	8.11	89.0	7.10	14.1
HyPR-SR gel	HyPR-gel **1**	9.1	40.2	97.6	28.8	3.47
	HyPR-gel **2**	13	29.6	96.7	22.0	4.55
	HyPR-gel **3**	18	26.5	96.4	18.3	5.46
	HyPR-gel **4**	36	16.7	94.3	13.1	7.63
	HyPR-gel **5**	54	15.2	93.8	12.4	8.06
	HyPR-gel **6**	73	10.1	91.0	8.64	11.6

3.3.2. Ionic conduction in SR gels containing in equilibrium swelling

AC impedance of neat IL **1**, PR-SR gel **1-6** and HyPR-SR gel **1-6** containing IL was measured. σ of the matrix without IL was less than 5×10^{-5} mS/cm, so the polymer matrix itself had very lower conductivity than that of IL. The conductivity spectra of PR- and HyPR-SR gels are shown in Fig. 3-3, respectively. The electrode polarization was observed in the low frequency region below 10^4 Hz, hence the

conductivity σ was estimated from the value around 10^5 Hz, where the conductivity did not have any dispersion.

(a)

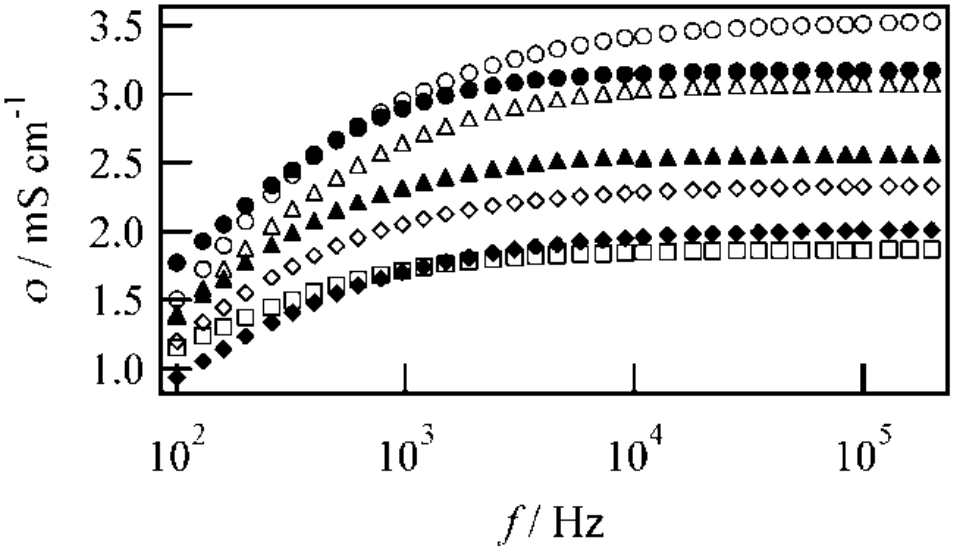

(b)

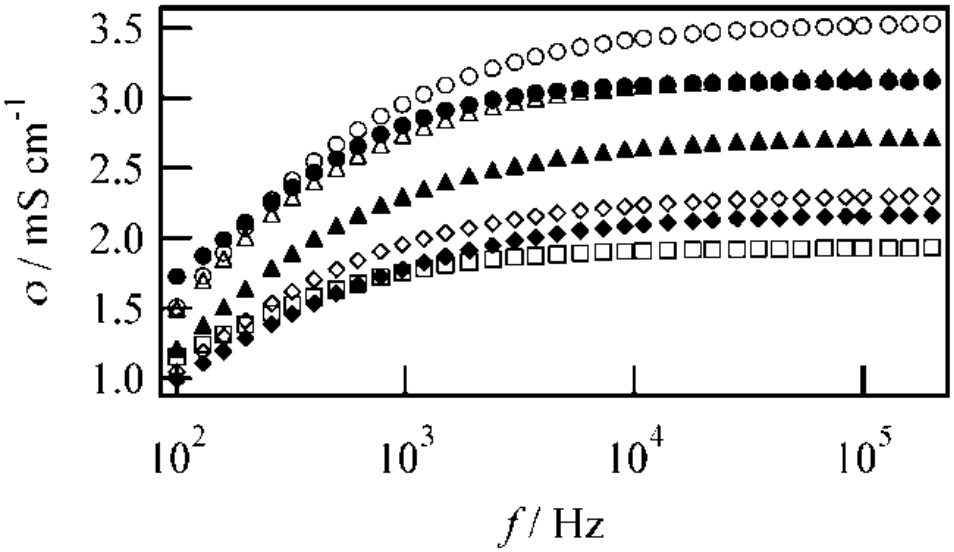

Fig.3-3. (a)Conductivity spectra of ionic liquid **1** (○), PR-gel **1** (●), PR-gel **2** (△), PR-gel **3** (▲), PR-gel **4** (◇), PR-gel **5** (◆), and PR-gel **6** (□). (b) Conductivity spectra of ionic liquid **1** (○), HyPR-gel **1** (●), HyPR-gel **2** (△), HyPR-gel **3** (▲), HyPR-gel **4** (◇), HyPR-gel **5** (◆), and HyPR-gel **6** (□).

Since the SR gel contained the PR network, which did not contribute to the ionic conduction, with a volume fraction of φ_v, σ was underestimated for the ionic conduction of IL in the SR gel. Hence, the molar conductivity Λ was adopted as per the following relation,

$$\Lambda = \sigma / \{2c_0(1-\varphi_v)\}, \quad (1)$$

where both the cation and anion contribute to the conductivity and c_0 is the concentration of neat ILs. In the case of IL **1**, c_0 was 5.25×10^{-3} mol cm^{-3}.

Table 3-3 shows σ, Λ, and the molar conductivity ratio of Λ to the molar conductivity of neat IL **1**, Λ_0 = 336 mS cm^2 mol^{-1}, of PR- and HyPR-SR gel and MMA gel with changing n. Since these molar conductivities were smaller than Λ_0 and conductivity decreased with n, it was suggested that the PR or HyPR network in the SR gel disturbed the ion transport. Generally, polymer networks in gels containing ILs disturbed the ionic transport of IL, and this result was consistent with previous reports [21-23]. However, Λ/Λ_0 was more than 92 % in PR-SR gel **1**, which was higher than the value in the previous report of gel containing IL [26-32], so hindrance of ion transport by PR or HyPR network in the SR gel was not very dominant in a high swelling ratio with a small cross-linking density.

On the other hand, a significant difference of ionic conductivities between PR- and HyPR-SR gels was not observed. This result was suggested that the swelling ratios of both gels were not far from.

Table 3-3. Conductivity σ of the SR gel and the MMA gel, molar conductivity Λ, and the molar conductivity ratio of Λ to the molar conductivity of neat IL **1** (Λ_0) of the ionic liquid in the SR gel in equilibrium swelling with changing number ratio of the cross-linking reagent n at 20 °C.

	No.	σ / mS cm^{-1}	Λ / mS cm^2 mol^{-1}	Λ / Λ_0 / %
Neat IL		3.53	336	100
PR-SR gel	PR-gel **1**	3.18	311	92.6
	PR-gel **2**	3.06	304	90.4
	PR-gel **3**	2.54	257	76.5
	PR-gel **4**	2.33	245	72.8
	PR-gel **5**	2.01	213	63.5
	PR-gel **6**	1.87	208	61.8
HyPR-SR gel	HyPR-gel **1**	3.12	308	91.5
	HyPR-gel **2**	3.13	312	92.9
	HyPR-gel **3**	2.70	272	81.0
	HyPR-gel **4**	2.30	237	70.5
	HyPR-gel **5**	2.16	224	66.6
	HyPR-gel **6**	1.66	179	53.3

3.3.3. Relation between mesh size and ionic conductivity of SR gel

After the ion conductivity measurements, the molecular weight between cross-links was estimated as follows. The SR gels swollen with IL **1** for the conductivity measurement were dipped in DMSO three times for 2 days for removing IL, and then dipped in methanol for exchanging the solvent, and dried in a vacuum chamber at 80 °C overnight. The weight of the dried gels was almost

invariant compared to that of the dried gels before swelling with IL. Further, PR- and HyPR-SR gels were swollen at equilibrium swelling with a good solvent of each SR gel, DMSO and Milli-Q water, respectively, and then the volume fraction φ_v' was estimated. The values of φ_v' were a little larger than those of φ_v estimated for swelling with IL, and it was found that the IL **1** can make the SR gel swell with a higher swelling ratio. The average molecular weight between cross-links M_c was calculated by the Flory-Rehner equation [33-34].

$$\frac{1}{M_c} = \frac{2}{M} - \frac{\ln(1-\phi_v') + \phi_v' + \chi_1 \phi_v'^2}{\left(\phi_v'^{1/3} - \phi_v'/2\right)} \frac{1}{\rho V_1}, \qquad (2)$$

where M is the molecular weight, χ_1 is the Flory-Huggins parameter, and V_1 is the molar volume of the solvent. In this analysis, we used the weight-averaged molecular weight of PEG, M_w (= 35,000), as the molecular weight M, because CDs scarcely contribute to the polymer conformation deciding the gel network swelling when the gel was swollen sufficiently. For the same reason, the Flory-Huggins parameters of PEG in DMSO (0.50) and in water (0.50) reported previously [35-36] were adopted as χ_1. The V_1 of DMSO and water was 71.0 cm^3 mol^{-1} and 18.0 cm^3 mol^{-1}, respectively, and ρ of PR and HyPR was estimated to be 0.99 g cm^{-3} and 0.92 g cm^{-3}, respectively. In Table 3-4, φ_v' measured in DMSO or water, M_c estimated by Eq. (2), and the average number of cross-links per PR or HyPR chain n_c are listed with changing n.

Since M_c was invariant with changing solvent from DMSO or water to the IL, the mesh size ξ of the PR- and HyPR-SR gel swollen with IL was estimated using the following relation [35,37].

$$\xi = \phi_{\mathrm{v}}^{-1/3} l_{\mathrm{c}} \sqrt{C_{\mathrm{n}} \frac{3M_{\mathrm{c}}}{M_{\mathrm{r}}}}, \qquad (3)$$

where φ_v is the volume fraction of PR in IL shown in Table 3-2, M_r is the molecular weight of the ethylene oxide unit, l_c (= 0.147 nm) is the average bond length of PEG, that is, the average length of C–C and C–O bonds, and C_n (= 3.8) is the characteristic ratio of PEG [35]. In this model, the PEG chain is regarded as a freely jointed chain with a segment length of l_c compensated by C_n. ξ estimated by Eq. (3) is also shown in Table 3-4.

Table 3-4. Volume fraction φ_v' measured in DMSO (PR-gels) or water (HyPR-gels), average molecular weight between cross-links M_c, average number of cross-links per PR or HyPR chain n_c, and mesh size ξ with changing number ratio of the cross-linking reagent *n*. cross-linking reagent *n* at 20 °C.

	No.	φ_v' / %	M_c / g mol^{-1}	n_c	ξ / nm
PR-SR gel	PR-gel **1**	3.16	17,300	3.13	45.9
	PR-gel **2**	4.62	17,100	3.21	38.9
	PR-gel **3**	6.62	16,400	3.36	34.3
	PR-gel **4**	8.85	15,200	3.88	31.0
	PR-gel **5**	16.9	8,860	4.27	21.2
	PR-gel **6**	20.4	6,450	6.43	16.2
HyPR-SR gel	HyPR-gel **1**	3.86	16,400	3.02	41.1
	HyPR-gel **2**	4.57	15,900	3.05	36.9
	HyPR-gel **3**	5.59	14,800	3.14	34.2
	HyPR-gel **4**	7.69	12,200	3.31	27.2
	HyPR-gel **5**	8.77	10,700	4.95	25.1
	HyPR-gel **6**	12.3	6,540	6.35	17.4

Comparing Table 3-3 and Table 3-4, it is seen that with decreasing mesh size, the molar conductivity decreased, and hence the SR gel network containing IL

disturbed the ionic conduction of IL. The diffusion constant D of a particle with a hydrodynamic radius R_H confined in a gel with a mesh size ξ can be approximately expressed as $D = D_0 \exp(-R_H/\xi)$, where D_0 is the intrinsic diffusion constant of the particle without gel network hindrance. By using the Nernst-Einstein relation, the molar conductivity can be written as

$$\Lambda = \Lambda_0 \exp(-R_H/\xi). \quad (4)$$

Figure 3-4 shows the relation between ξ^{-1} and $\ln(\Lambda/\Lambda_0)$ of PR- and HyPR-SR gel. An approximate linear relation can be confirmed for both types of SR gel, and from the slope of the fitting line, the hydrodynamic radius of the ionic motion unit R_H was estimated to be 9.7 nm. Since the ion radius of IL **1** was reported to be 0.3 nm [38], the radius obtained in this study was larger than the single ion radius, and hence the result indicated that ions were transported hydrodynamically in relatively stable aggregates with radius about 30 times larger than that of a single ion. This tendency has been reported previously and our result was consistent with those reports [39-40].

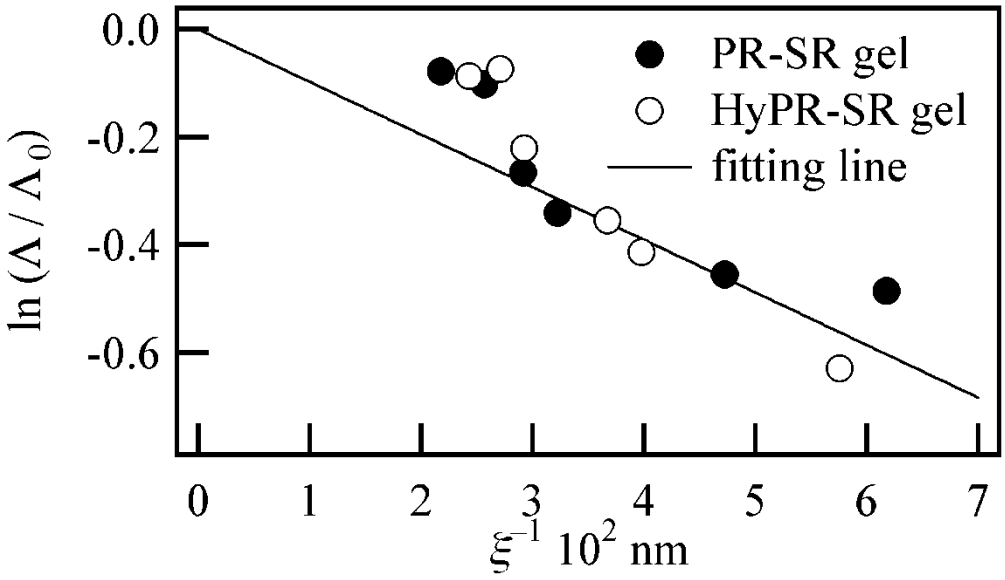

Fig. 3-4. The relation between ξ^{-1} and $\ln(\Lambda/\Lambda_0)$ for the PR- and HyPR-SR gels.

3.3.4. Conductivity of SR gel under compressive deformation

A large deformation of gels induces deformation of polymer networks, which is expected to affect ionic conduction. Hence, we applied compressive deformation to the SR gels and measured the ionic conduction. In this study, the average molecular weight between cross-links M_c was estimated by elasticity measurement instead of the Flory-Rehner equation, since all of the gels were not in an equilibrium swelling condition. First, PR- and HyPR-SR gel **7**, **8** were swollen with mass fraction of PR or HyPR of about 10 wt% using a good solvents for each SR gel, DMSO and Milli-Q water, respectively, and we measured the elasticity. While, it is difficult to remove IL from MMA gel **1**, **2**, hence the MMA gels were used in the condition swollen with IL **9**. Figure 3-5 shows the dynamic storage elastic modulus $E(f)$ of PR- and HyPR-SR gel **7**, **8**, and MMA gel **1**, **2**. All the samples showed a plateau in the frequency region from 0.1 to 10 Hz, and $E(f)$ in this region was adopted as the

storage elastic modulus E. Gels with large cross-linking density tended to have a large E, and M_c was estimated using the relation [33,41]:

$$\frac{1}{M_c} = \frac{2}{M} + \frac{E'}{3\rho RT}, \qquad (5)$$

where M is the molecular weight and ρ is the density of the gels. The weight-averaged molecular weight of PEG, M_w (= 35,000), was used as M on PR- and HyPR-SR gels, and the value (of 29,000) synthesized using the same conditions reported previously [42] was used for the MMA gels. The solvent densities of DMSO (1.10 g m^{-3}) on PR-, water (1.00 g m^{-3}) on HyPR-, and ionic liquid **9** (1.52 g m^{-3}) on MMA gels were used as ρ. Table 3-5 shows the volume swelling ratio for swelling with IL, Q_v, the volume fraction for swelling with IL, φ_v, the elastic modulus measured in the condition mentioned above, E', and the average molecular weight between cross-links estimated by Eq. (5), M_c of the SR and MMA gels. The results showed that all gels have similar values of φ_v and M_c.

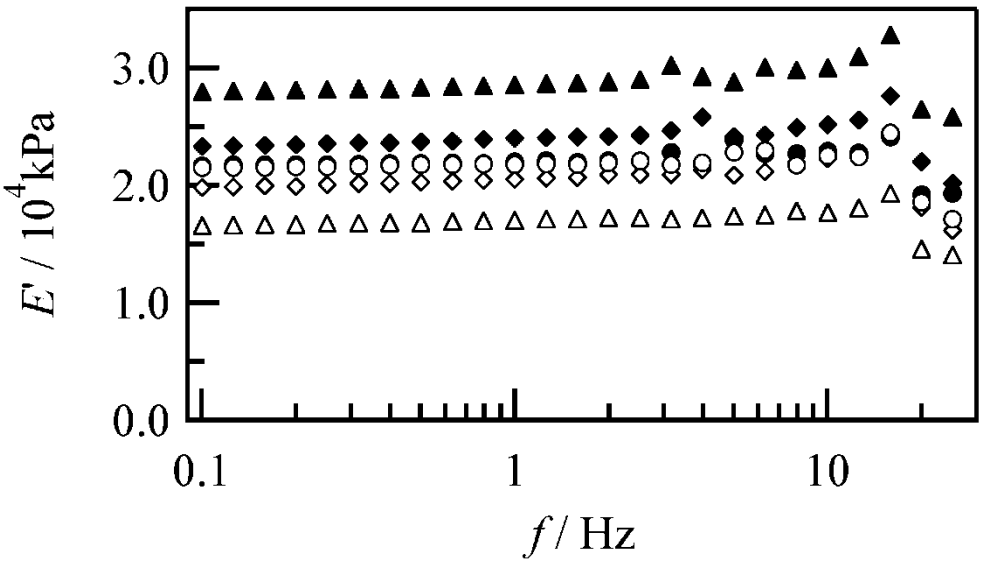

Fig. 3-5. Dynamic storage elastic modulus $E(f)$ of PR-gel 7 (○), PR-gel 8 (●), HyPR-gel **7** (△), HyPR-gel **8** (▲), MMA gel **1** (◇), and MMA gel **2** (◆).

Table 3-5. The volume swelling ratio swollen with ionic liquid, Q_v, volume fraction swollen with ionic liquid, φ_v, elastic modulus measured in the condition mentioned above, E, and average molecular weight between cross-links estimated by Eq. (5), M_c of the SR and MMA gels.

	No.	Q_v	φ_v / %	E / kPa	M_c / g mol^{-1}
PR-SR gel	PR-gel **7**	7.60	13.2	22.0	16,700
	PR-gel **8**	7.59	13.2	22.2	16,586
HyPR-SR gel	HyPR-gel **7**	7.60	13.2	17.0	16,806
	HyPR-gel **8**	7.59	13.2	27.7	16,420
MMA gel	MMA gel **1**	–	12.5	21.0	14,586
	MMA gel **2**	–	12.5	25.3	14,504

Compressing each gel, ionic conductivity measurements in the direction of compressive deformation was performed. Figure 3-6 shows the conductivity σ reduced by the conductivity without any compression σ_0 with changing compression ratio λ of PR-gel **8** and MMA gel **2**. In both gels, σ/σ_0 increased with λ in the low

compression region. In the case of the MMA gel **2**, σ/σ_0 showed a peak at λ of about 0.70 and the gel was then crushed at a λ of about 0.64. This tendency was almost same as the MMA gel **1**, so behavior for a high compression ratio less than 0.6 could not be investigated in the MMA gel synthesized under the condition used in this study. On the other hand, in the case of PR-gel **8**, σ/σ_0 showed a peak at a λ of about 0.75 that then decreased to 0.80 at a λ of about 0.33, and the gel was not crushed in the compression region investigated in this study. This tendency was also the same as for PR-gel **7**. In the case of HyPR-gel **7** and **8**, the increment of σ/σ_0 was scarcely observed, that is, σ/σ_0 remained almost constant in the low compression region, and then the value decreased in a similar manner as PR-gel **8**. PR- or HyPR-gel were not crushed in the compression regime used in this study. This resistance characteristic against compressive deformation may be a unique property of the slide-ring gel with movable cross-links that can relax tensile stress.

Fig. 3-6. The conductivity σ reduced by that without compression σ_0 with changing compression ratio λ of PR-gel **8** (○) and MMA gel **2** (△).

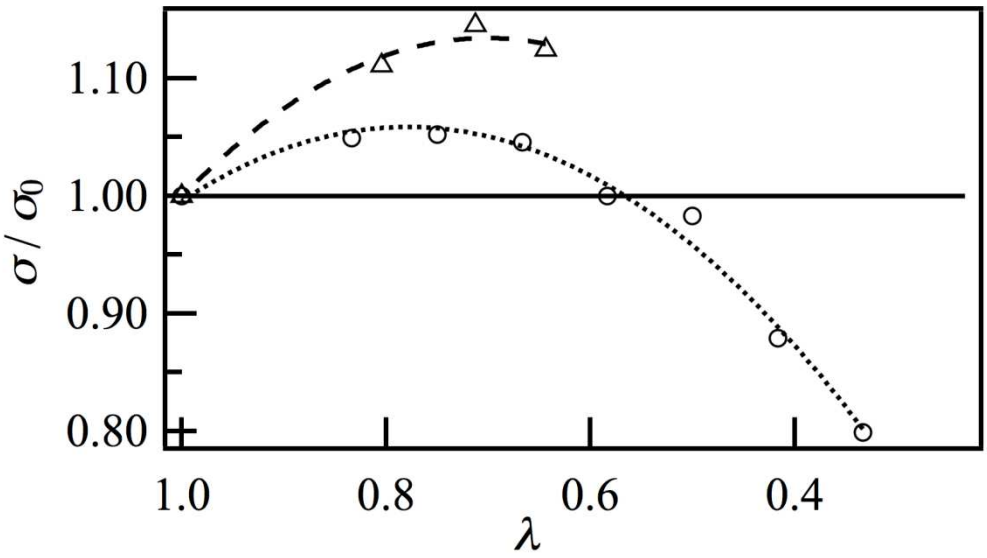

For explaining the conductivity change under compression, we suggested the following model. The gel network was regarded as a stack of mesh sheets with mesh size l_x and l_y and with interval l_z as shown in Fig. 3-7. Compression was applied to the stacking direction of the mesh sheets. At first, in the low compression region, $\lambda > 0.6$, the mesh sheet was spread out perpendicular to the compressed direction and l_x, l_y increased. Since the ionic conduction was measured along the compressed direction, ionic carriers can be transported more freely without disturbing the mesh sheet as shown in Fig. 3-7 (a), hence σ/σ_0 increased with λ. In the high compression region, $\lambda < 0.6$, the mesh sheet was also spread out, however, the distance between the mesh sheets decreased by compression deformation and l_z then became of a comparable size to R_H as shown in Fig. 3-7 (a). Since l_x, l_y and l_z without compression were estimated to be about 26 nm from Eq. (3), l_z of the

compressed gel with $\lambda = 0.5$ was roughly estimated to be 13 nm, and this length was comparable to R_H. In this case, the translational motion of ionic carriers parallel to the mesh sheet was restricted by pressure from the forward and backward mesh polymers, so carriers cannot escape from the hindrance caused by the mesh when the carriers got stuck in the mesh as shown in Fig. 3-7 (b). Accordingly, σ/σ_0 decreased with λ in this region.

(a)

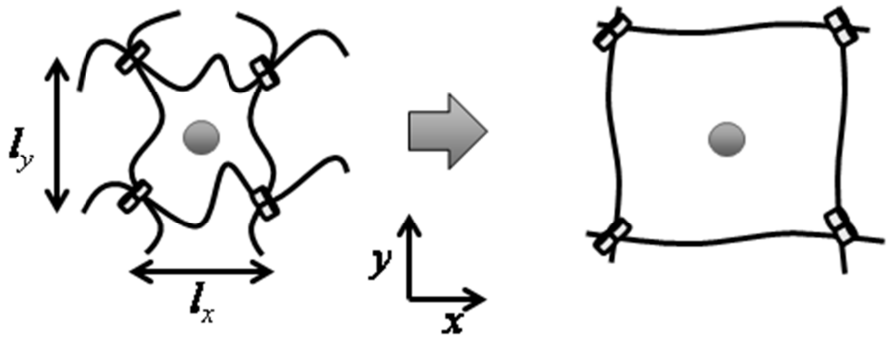

(b)

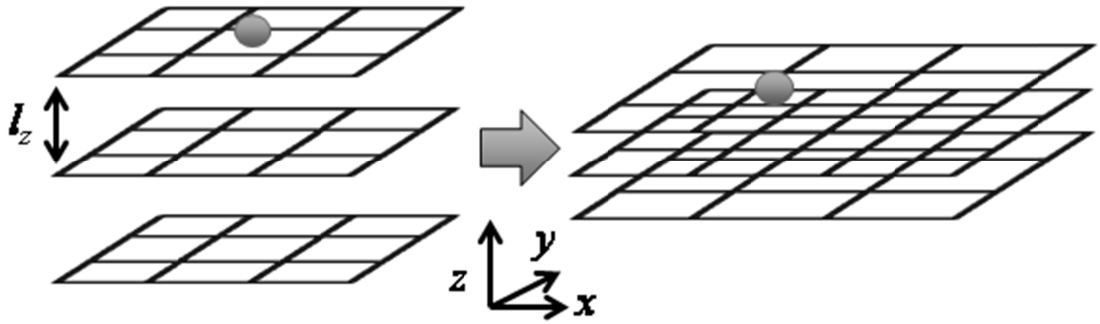

Fig. 3-7. Schematic images of the SR gel network before/after compressive deformation. (a) The network within the *xy* plane was regarded as the mesh sheet with mesh size l_x and l_y with compression along the *z* direction. (b) The network was regarded as a stack with interval l_z of the mesh sheets, where the linkages between the meshes and cross-linking CDs are not shown for simplicity.

3.4. Summary

The molar conductivity of SR gel swollen with 1-ethyl-3-methylimidazolium ethylsulfate (EMIES) was more than 92 % of that of neat IL with high swelling ratio with a small cross-linking density, and hence ionic transport was found to be almost free of the polymer networks of the SR gel. With increasing cross-linking density,

the swelling ratio and molar conductivity decreased due to increasing disturbance of ion transport by the polymer networks, and the hydrodynamic radius of the ionic motion unit was estimated to be 9.7 nm. Further, with compressive deformation, at first the polymer network was spread out perpendicular to the compressed direction and ionic carriers were transported more freely without interference from the network. Then, with increasing compressive deformation, from the pressure of the polymer network along the compressed direction, ionic carriers could not escape from the polymer network hindrance and the conductivity decreased.

References

[1] J. Dupont, R. F. de Souza, P. A. Z. Suarez, Ionic liquid (molten salt) phase organometallic catalysis, Chem. Rev. 102 (2002) 3667-3692.

[2] T. Walton, Room-temperature ionic liquids. solvents for synthesis and catalysis, Chem. Rev. 99 (1999) 2071-2084.

[3] P. Wasserschied, W. Keim, Ionic liquids-new “solutions” for transition metal catalysis, 39 (2000)3772-3789.

[4] R. Sheldon, Catalytic reactions in ionic liquids, Chem. Commun. 23 (2001) 2399-2407.

[5] K. R. Seddon, Ionic liquids: a taste of future, Nat. Mater. 2 (2003) 363-365.

[6] W. Xu, C. A. Angell, Solvent-free electrolytes with aqueous solution-like conductivities, Science 302 (2003) 422-425.

[7] J. Fuller, A. C. Breda, R. T. Carlin, Ionic liquid-polymer gel electrolytes from hydrophilic and hydrophobic ionic liquids, J. Electroanal. Chem. 459 (1998) 29-34.

[8] H. Nakagawa, S. Izuchi, K. Kuwana, T. Nukuda, Y. Aihara, Liquid and polymer gel electrolytes for lithium batteries composed of room-temperature moltensalt doped by lithium salt, J. Electrochem. Soc. 150 (2003) A695-A700.

[9] A. Lewandowski, A. Swiderska-Mocek, Ionic liquids as electrolytes for Li-ion batteries-an overview of electrochemical studies, 194 (2009) 601-609.

[10] A. B. McEwen, S. F. McDevitt, V. R. Koch, Nonaqueous electrolytes for electrochemical capacitors: imidazolium cations and inorganic fluorides with organic carbonates, J. Electrochem. Soc. 144 (1997) L84-L86.

[11] M. Ue, M. Takeda, A. Toriumi, A. Kominato, R. Hagiwara, Y. Ito, J. Electrochem. Soc. 150 (2003) A499-A502.

[12] T. Sato, G. Masuda, K. Takagi, Electrochemical properties of novel ionic liquids for electric double layer capacitor applications, Electrochem. Acta 49 (2004) 3603-3611.
[13] P. Wang, S. M. Zakeeruddin, J. E. Moser, M. Gratzel, A new ionic liquid electrolyte enhances the conversion efficiency of dye-sensitized solar cells, J. Phys. Chem. B 107 (2003) 13280-13285.
[14] W. Kubo, T. Kitamura, K. Hanabusa, Y. Wada, S. Ynagida, Quasi-solid-state dye-sensitized solar cells using room temperature molten salts and a low molecular weight gelator, Chem. Commun. (2002) 374-374.
[15] N. Kimizuka, T. Nakashima, Spontaneous self-assembly of glycolipid bilayer membranes in sugar-philic ionic liquids and formation of ionogels, Langmuir, (2001) 6759-6761.
[16] K. Hanabusa, H. Fukui, M. Suzuki, H. Shirai, Specialist gelator for ionic liquids, Langmuir 21 (2005) 10383-10390.
[17] H. yang, C. Yu, Q. Song, Y. Xia, F. Li, Z. Chen, X. Li, T. Yi, C. Huang, High-temperature and long-term stable solid-state electrolyte for dye-sensitized solar cells by self-assembly, Chem. Mater. 22 (2006) 5173-5177.
[18] T. Fukushima, A. Kosaka, Y. Ishimura, T. Yamamoto, T. Takigawa, N. Ishii, T. Aida, Molecular ordering of organic molten salts triggered by single-walled carbon nanotubes, Science 300 (2003) 2072-2074.
[19] Y. Zhang, Y. Shen, J. Li, L. Niu, S. Dong, A. Ivaska, Electrochemical functionalization of single-walled carbon nanotubes in large quantities at a room-temperature ionic liquid supported three-dimensional network electrode, Langmuir 21 (2005) 4797-4800.
[20] P. Yu, J. Yan, H. Zhao, L. su, J. Zhang, L. Mao, Rational functionalization of carbon nanotube/ionic liquid bucky gel with dual tailor-made electrocatalysts for four-electron reduction of oxygen, J. Phys. Chem. C, 112 (2008) 2177-2182.
[21] T. Ueki, M. Watanabe, Macromolecules in ionic liquids: progress, challenges, and opportunities, Macromolecules 41 (2008) 3739-3749.
[22] A. Noda, M. Watanabe, Highly conductive polymer electrolytes prepared by in situ polymerization of vinyl monomers in room temperature molten salts, Electrochim. Acta 45 (2000) 1265-1270.
[23] M. A. B. H. Susan, T. Kaneko, T. Ueki, M. Watanabe, Ion gels prepared by in situ radical polymerization of vinyl monomers in an ionic liquid and their characterization as polymer electrolytes, J. Am. Chem. Soc. 127 (2005) 4976-4983.
[24] N. Murata, A. Konda, K. Urayama, T. Takigawa, M. Kidowaki, K. Ito, Anomaly in stretching-induced swelling of slide-ring gels woth movable cross-links, Macromolecules

42 (2009) 8485-8491.
[25] S. Samitsu, J. Araki, T. Kataoka, K. Ito, New solvent for polyrotaxane. II. Dissolution behavior of polyrotaxane in ionic liquids and preparation of ionic liquid-containing slide-ring gels, J. Polym. Sci. Part B 44 (2006) 1985-1994.
[26] S. A. Chesnokov, M. Y. Zakharina, A. S. Shaplov, E. I. Lozinskaya, I. A. Malyshkina, G. A. Abakumov, F. Vidal, Y. S. Vygodskii, Photopolymerization of poly(ethylene glycol) dimethacrylates: the influence of ionic liquids on the formulation and the properties of the resultant polymer materials, J. Polym. Sci. Part A 48 (2010) 2388-2409.
[27] H. Nakajima, H. Ohno, Preparation of thermally stable polymer electrolytes from imidazlium-type ionic liquid derivatives, Polymer 46 (2005) 11499-11504.
[28] M. A. Klingshrin, S. K. Spear, R. Subramanian, J. D. Holbrey, J. G. Huddleston, R. D. Rogers, Gelation of ionic liquids using a cross-linked poly(ethylene glycol) gel matrix, Chem. Mater. 16 (2004) 3091-3097.
[29] F. Vidal, C. Plesse, D. Teysie, C. Chevrot, Long-life air working conducting semi-IPN/ionic liquid based actuator, Synth. Met. 142 (2004) 287-291.
[30] M. A. Neouze, J. L. Bideau, P. Gaveau, S. Bellayer, A. Vioux, Ionogels, New materials arising from the confinement of ionic liquids qithin silica-derived networks, Chem. Mater. 18 (2006) 3931-3936.
[31] K. Matsumoto, S. Sogabe, T. Endo, Synthesis and properties of methacrylate –based networked polymers having ionic liquid structures, J. Polym. Sci. Part A 48 (2010) 4515-4521.
[32] T. Kawauchi, M. Ohara, S. Hirai, T. Takeichi, Preparation of polybenzoxazine/ionic liquid hybrids, Chem. Let. 37 (2008) 1132-1133.
[33] J. He, K. Horie, R. Yokota, Characterization of polyimide gels crosslinked with hexamethylene diisocyanate, Polymer 41 (2000) 4793-4802.
[34] J. B. Thomas, J. H. Tingsanchali, A. M. Rosales, C. M. Cresscy, J. W. McGinity, N. A. Peppas, Polymer 48 (2007) 5042-5048.
[35] J. B. Thomas, J. H. Tingsanchali, A. M. Rosales, C. M. Creecy, J. W. McGinity, N. A. Peppas, Dynamics of poly(ethylene glycol)-tethered, pH responsive networks, Polymer 48 (2007) 5042-5048.
[36] C. O. Dinc, G. Kibarer, A. Guner, Solubility profiles of poly(ethylene glycol)/solvent systems. II. comparison of thermodynamic parameters from viscosity measurements, J. Appl. Polym. Sci. 117 (2010) 1100-1119.
[37] B. Kim, N. A. Peppas, Synthesis and characterization of pH-sensitive glycopolymers for oral drug delivery systems, J. Biomater. Sci. Polym. Ed. 13 (2002) 1271-1281.

[38] 川野 竜司, 徳田 浩之, 片伯部 貫, 中本 博文, 小久保 尚, 今林 慎一郎, 渡邉 正義, イオン液体及びイオンゲル中の特異的電荷輸送とその材料科学的重要性, Kobunshi Ronbunshu 63 (2006) 31-40
[39] A. Noda, K. Hayamizu, M. Watanabe, Pulsed-gradient spin echo ^{1}H and ^{19}F NMR ionic diffusion coefficient, viscosity, and ionic conductivity of non-chloroaluminate room-temperature ionic liquids, J. Phys. Chem. B 105 (2001) 4603-4610.
[40] M. Galinski, A. Lewandowski, I. Stepniak, Ionic liquids as electrolytes, Electrochim. Acta 51 (2006) 5567-5580.
[41] A. V. Tobolsky, D. W. Carlson, N. Indictor, Rubber elasticity and chain configuration, J. Polym.. Sci. Part A 54 (1961) 175-192.
[42] S. M. Lomakin, J. E. Brown, R. S. Breese, M. R. Nyden, An investigation of the thermal stability and char-forming tendency of cross-linked poly(methyl methacrylate), Polym. Degrad. Stab. 41 (1993) 229-243.

Chapter 4

Ion-conductive and Mechanical Properties of Slide-Ring Gels Swollen with Ionic Liquid with Lithium Salts

4.1. Introduction

Typically electrolyte solutions (ES) for lithium ion batteries consisted of an organic solvent and lithium salt, however, these ESs have inflammability which is the cause of ignited or exploded. Hence, the characteristics of ionic liquid (IL) [1-5] such as negligible vapor pressure and non-flammability, are attracted to resolve the problems for safety. Neat ILs can be applied on ES for electric double-layer capacitor which is not needed specific ion species [6-7], however, ES for lithium ion battery is necessary containing lithium salt to provide the electroactive species.

Generally, with lithium concentration, the ionic conductivity of organic solvent including lithium ion increased, and then decreased, on the other hand, that of IL including lithium ion decreased with increasing lithium ion concentration [8]. This is suggested that electrostatic interaction and viscosity increased with lithium ion concentration while neat IL is the concentrated solution. However, the room temperature ionic conductivity of IL including lithium ion has close to that of organic solvent, therefore, these characteristics of ILs were expected to be improve lithium ion batteries satisfying requirements for more safety and higher electrochemical performance [9-12].

In this chapter, we investigated the unique swelling behavior and ionic conduction of SR gels swollen with IL including various lithium ion densities. Furthermore, we report puncture measurements of swollen gels to investigate the mechanical properties of the SR gel network swollen with IL and lithium ion mixture.

4.2. Experimental

4.2.1. Materials

Hydroxypropyl PR (HyPR), in which α-CDs are threaded by PEG (M_w = 35,000) and ca. 50% of the hydroxyl groups of α-CDs in PR were modified by hydroxypropyl groups, was purchased from Advanced Softmaterials Co., Ltd. According to the information provided by the manufacturer, the number of α-CD rings included in a single PR molecule is estimated to be ca. 98 from ^{1}H nuclear magnetic resonance spectroscopy (NMR) measurements, which corresponds to a stoichiometric α-CD to ethylene oxide unit ratio of 1:8.1 (inclusion ratio = 24.7%) in the inclusion complex. Divinyl sulfone (Tokyo Chemical Industry Co., Ltd.) was used as a cross-linker without further purification. Dehydrated dimethyl sulfoxide (DMSO), dehydrated dimethyl formamide (DMF) and dichloromethane, which were used to wash the SR gels, were purchased from Wako Pure Chemical Industries, Ltd. and used without further purification. A mixture of 1-ethyl-3-methylimidazolium bis(trifluoromethanesulfonyl)imide (EMITFSI) and lithium bis(trifluoromethanesulfonyl)imide (LiTFSI) was purchased from Kishida Chemical Co., Ltd. and used as the ES without further purification.

4.2.2. Preparations of SR gels

HyPR (50.0 mg, 2.73×10^{-7} mol for swelling and electrochemical measurement; 133.4 mg, 7.28×10^{-7} mol for mechanical measurement) was dissolved in 1.0 M NaOH aqueous solution (333 μL for swelling and electrochemical measurement; 900 μL for mechanical measurement), and the same method and cross-linking agents for cross-linking, which were explained in section 2.2.3, was

applied. After vortex mixing for 30 min in an ice bath, the samples were poured into Teflon® spacers with a width of 500 μm, degassed under vacuum, and settled for 24 h in a refrigerator to obtain HyPR-SR gels. The SR gels were immersed in deionized water, dehydrated DMSO, dehydrated DMF and dichloromethane, each three times for 3 h to remove any residual impurities and solvent, and then dried at 353 K in a vacuum chamber overnight. The dried HyPR-SR gels were then swollen in an ES composed of 0.5 to 1.0 M LiTFSI in EMITFSI for 7 days in a glovebox under a dry N_2 atmosphere to achieve equilibrium swelling.

Non-equilibrium swollen gels were prepared with HyPR-SR gels crosslinked with a 6.0% ratio of divinyl sulfone in the same way as that for the equilibrium swollen gels. The dried HyPR-SR gels were swollen in 0.8 M ES for 0 to 7 days in a glovebox under a dry N_2 atmosphere, and the gels were then removed from the ES solution before equilibrium swelling was achieved.

The weight-swelling ratio Q_w, is defined as $Q_w = W/W_0$, where W_0 is the weight of the dried gel before swelling with ES, and W is the weight of the gel after swelling with ES. The volume swelling ratio Q_v, is defined as $Q_v = (L/L_0)^3$, where L_0 is the edge length of the dried gel before swelling with ES, and L is the length of the gel after swelling, assuming that swelling occurs isotropically. All measurements were performed in a glovebox under a dry N_2 atmosphere.

4.2.3. ATR measurements

Attenuated total reflectance-Fourier transform infrared (ATR-FTIR; FT/IR-4100, JASCO Corporation) spectroscopy measurements were performed to analyze complexation of lithium cations, the ether oxygen atoms on HyCDs and

TFSI anions at 298 K in an air atmosphere.

4.2.4. Ionic conductivity measurement

AC impedance measurements were performed to investigate the ionic conductivity of pristine ES and the SR gels swollen with ES. Pristine ES was filled in a coin cell (CR 2032, AA Portable Power Corporation). The gel was cut to a thickness of 5.00×10^{2} μm and an area of 0.282 cm^{2}, and then sandwiched with a Teflon® spacer between two stainless-steel plates held together with a clip. AC impedance measurements of the pristine ES were performed using a potentiostat/galvanostat meter (SP-200, Bio-Logic, Inc.) within the frequency range of 10^{2}–10^{5} Hz and from 303 to 373 K in 10 K increments, while measurements of the SR gels swollen with ES were performed using a potentiostat/galvanostat meter (SP-150, Bio-Logic, Inc.) within the frequency range of 10^{2}–10^{5} Hz under a dry Ar atmosphere in a glovebox from 293 to 373 K in 10 K increments.

4.2.5. Mechanical measurement

Stress-strain measurements were conducted by puncture testing to investigate the mechanical characteristics of the equilibrium and non-equilibrium swollen HyPR-SR gels. This measurement method is used commonly in product development at many companies. Stress-strain curves were measured for fixed HyPR-SR gel punctured with a 1.0 mm diameter pin with a tip radius of 0.5 mm (TKS-250N, Imada Co., Ltd.) at a rate of 50 mm/s. The measurement was performed using a universal tensile testing machine (Tensilon RTC-1250, Orientec Co., Ltd.) in air at room temperature.

The actual stress exerted to a gel cannot be directly obtained by the puncture measurement, because the gel is elongated cylindrically to wrap the pin, so that the cross section to which the force is exerted does not correspond to the tip area of the pin. Therefore, the puncture stress σ_t, and the puncture elongation ε, were defined using the incompressible assumption, $\pi a^2 d \simeq \pi(\chi^2 - a^2)L$, as follows:

$$\sigma_t = f/\{\pi(\chi^2 - a^2)\} \simeq fL/(\pi a^2 d), \quad (1)$$

$$\varepsilon = (L + a)/a \simeq L/a, \quad (2)$$

where f is the applied force, L is the displacement of the tip, a is the tip radius of the pin, and d is the original thickness of the gel, as shown in Fig. 4-1. This model can only be applied under large deformation; therefore, Young's modulus E, defined under small deformation, was estimated from the stress and strain detected with the tensile testing machine.

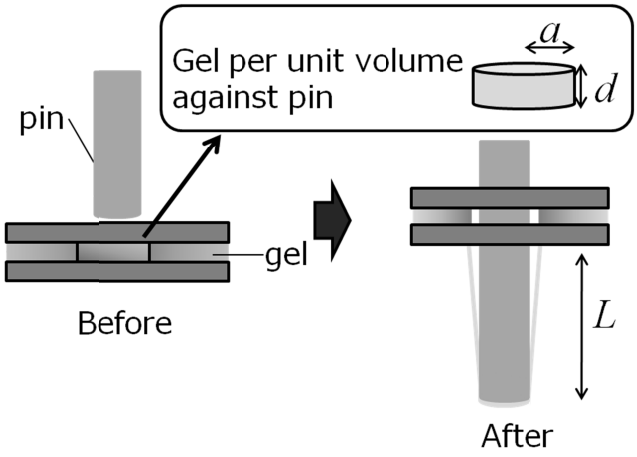

Fig. 4-1. Puncture measurement analysis method.

4.3. Results and discussion

4.3.1. Structure analysis by ATR-IR

ATR-FTIR analysis was conducted for HyPR, pristine ES of 1.5 M lithium ion density, and their mixture. Figure 4-2 shows ATR-FTIR spectra for HyPR, pristine ES, and the ES:HyPR mixture (500:55.8 mg). The spectrum for HyPR had absorptions at 3331 cm^{-1} (O−H of CD), 2916 and 2873 cm^{-1} (CH_2 of PEG and CD), 1641 cm^{-1} (broad, amide), 1480-1240 cm^{-1} (C−H bending and O−H in-plane bending from CD), 1150 cm^{-1} (O−H bending or coupled C−O stretching of CD), 1078 and 1027 cm^{-1} (C−C or C−O stretching of CD), 949, 938, 751, 702, 605, and 572 cm^{-1} (ring vibration of CD), and 860 cm^{-1} (C_1 group vibration of CD), which were consistent with that reported previously [13]. The ATR-FTIR peaks that correspond to pristine ES were observed at 3200-3100 cm^{-1} (ring C−H stretch), 3000-2900 cm^{-1} (C−H stretch), 1571 cm^{-1} (C=N stretch), 1460 cm^{-1} (C=C stretch), 1344 and 1330 cm^{-1} (C−N stretch), 1230-1130 cm^{-1} (C−F stretch), and 1052 cm^{-1} (S=O bending), which were also consistent with that reported previously [14]. The spectrum for the ES:HyPR mixture had a broad peak at 3520 cm^{-1}, in addition to the peaks observed for both HyPR and pristine ES. The peak for HyPR at 3331 cm^{-1} (O−H of CD) was shifted to higher wavenumber in the mixture, which suggests that intermolecular hydrogen bonds between the hydroxyl groups of CDs were broken by the formation of coordination bonds between lithium cations and ether oxygen atoms on CDs [15].

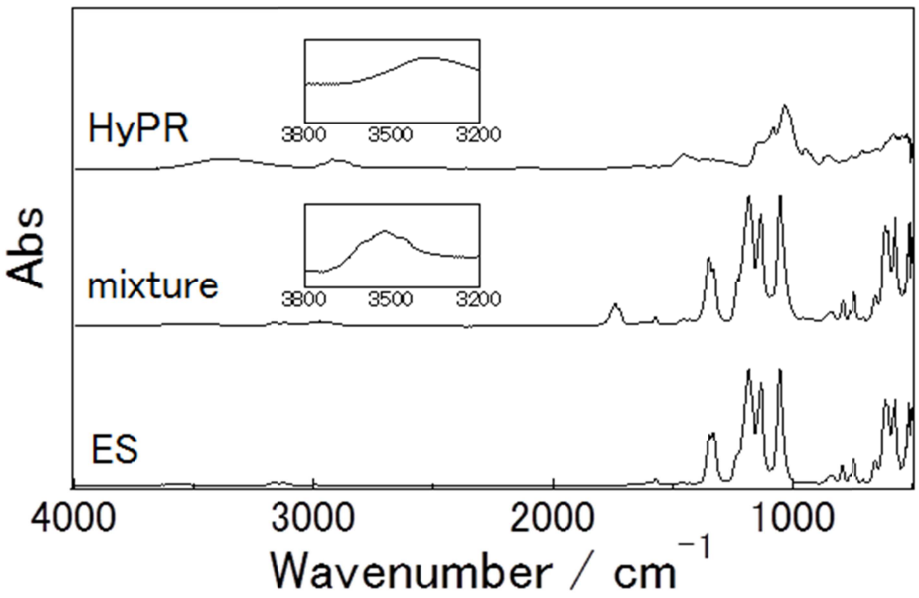

Fig. 4-2. ATR-FTIR spectra for HyPR powder, 1.5 M ES, and a mixture of the HyPR powder and ES.

4.3.2. Equilibrium and non-equilibrium swelling behavior

Table 4-1 shows L_0 and L for the ESs, estimated Q_w and Q_v, and the volume fraction occupied by PR φ_v, in the HyPR-SR gels swollen with ES at equilibrium. Each gel was prepared with a different lithium ion density c, and a different ratio n, of the cross-linking reagent to the sum of the hydroxyl and hydroxypropyl groups of HyCD. In chapter 2.3.1, we explained that the HyPR-SR gel could not swollen with the pure IL due to the different affinity of the hydrophilic PR and the hydrophobic IL, whereas these gels did exhibit swelling behavior in the ES. To confirm the relation between the swelling ratio and swelling time, W_0 and W for the ES, and the estimated Q_w are given in Table 4-2 for the ES with a lithium ion density of 0.8 M was used. The gels were swollen rapidly to equilibrium within 2 days and those gels that reached equilibrium swelling did not reduce their retention volumes with an

increase in the swelling time.

Table 4-1. Weight Q_w, and volume Q_v, swelling ratios, and volume fraction φ_v, of HyPR-SR gels immersed in ES as solvents for equilibrium swelling with various cross-linking reagent number ratio n, and various lithium ion density, c.

c / mol L^{-1}	n / %	No.	L_0 / mm	L of ES / mm	Q_w of ES	Q_v of ES	φ_v / %
0.5	10	HyPR-SR gel **1**	9.8	15.8	8.7	4.2	24.0
	9.0	HyPR-SR gel **2**	7.8	16.3	10.0	9.1	11.0
	8.0	HyPR-SR gel **3**	10.3	165	12.3	4.1	24.5
	7.0	HyPR-SR gel **4**	9.8	17.2	13.6	5.4	18.5
	6.0	HyPR-SR gel **5**	9.5	17.7	16.8	6.4	15.6
0.6	10	HyPR-SR gel **6**	9.0	16.1	11.1	5.8	17.3
	9.0	HyPR-SR gel **7**	8.5	15.9	11.3	6.5	15.3
	8.0	HyPR-SR gel **8**	8.9	17.2	14.3	7.2	13.9
	7.0	HyPR-SR gel **9**	9.2	17.8	15.5	7.3	13.8
	6.0	HyPR-SR gel **10**	9.4	19.0	14.8	8.3	12.0
0.7	10	HyPR-SR gel **11**	9.7	17.5	15.5	5.9	17.9
	9.0	HyPR-SR gel **12**	9.4	17.6	16.4	6.4	15.5
	8.0	HyPR-SR gel **13**	9.7	19.8	17.8	8.4	11.8
	7.0	HyPR-SR gel **14**	9.6	18.2	20.1	7.0	14.3
	6.0	HyPR-SR gel **15**	7.8	17.0	22.7	10.4	9.62
0.8	10	HyPR-SR gel **16**	9.5	20.3	24.1	9.7	10.3
	9.0	HyPR-SR gel **17**	8.6	20.0	24.8	12.5	8.02
	8.0	HyPR-SR gel **18**	8.6	19.2	22.4	11.1	9.02
	7.0	HyPR-SR gel **19**	9.7	21.2	29.1	10.4	9.58
	6.0	HyPR-SR gel **20**	9.4	20.7	31.1	10.9	9.18

c / mol L^{-1}	n / %	No.	L_0 / mm	L of ES / mm	Q_w of ES	Q_v of ES	φ_v / %
0.9	10	HyPR-SR gel **21**	8.7	16.9	12.6	7.3	14.2
	9.0	HyPR-SR gel **22**	8.6	16.8	15.1	7.6	13.3
	8.0	HyPR-SR gel **23**	8.6	17.6	15.9	8.4	12.1
	7.0	HyPR-SR gel **24**	9.3	19.7	17.0	9.5	10.3
	6.0	HyPR-SR gel **25**	8.7	19.1	19.1	10.6	9.61
1.0	10	HyPR-SR gel **26**	9.9	16.9	10.9	5.1	19.7
	9.0	HyPR-SR gel **27**	9.6	16.6	11.9	5.2	19.2
	8.0	HyPR-SR gel **28**	9.0	17.4	13.2	7.1	14.1
	7.0	HyPR-SR gel **29**	9.3	18.2	13.7	7.6	13.1
	6.0	HyPR-SR gel **30**	9.6	18.8	15.0	7.7	13.0

Table 4-2. Swelling time and weight swelling ratio Q_w, for HyPR-SR gels prepared with 0.8 M ES.

Swelling time / day	No.	W_0 / mg	W of ES / mg	Q_w of ES
0	HyPR-SR gel **31**	89.8	89.8	1
1	HyPR-SR gel **32**	95.6	893.4	9.35
2	HyPR-SR gel **33**	89.6	1307.6	14.6
3	HyPR-SR gel **34**	72.8	1116.2	15.3
4	HyPR-SR gel **35**	75.8	1120.3	14.8
5	HyPR-SR gel **36**	83.6	1271.0	15.2
6	HyPR-SR gel **37**	91.9	1354.8	14.7
7	HyPR-SR gel **38**	93.1	1371.3	14.7

Furthermore, Fig. 4-3 shows the relation between c and Q_V. At low lithium ion density, the swelling ratio increased with the lithium ion density, whereas at high lithium ion density, the swelling ratio decreased with an increase in the lithium ion density. Therefore, dependence of the swelling ratio on the lithium ion density was convex upward with the maximum peak at 0.8 M. For lithium ion densities below 0.8 M, this tendency is suggested to be due to a solvation effect by the formation of coordination bonds between PR and lithium ions in the IL, which is consistent with the ATR-FTIR results. Above 0.8 M, the tendency for the swelling ratio to decrease with c suggests the formation of physical cross-linkages between PR molecules by lithium cations. A lithium cation can form coordination bonds with a few oxygen atoms of HyCDs; therefore, this structure can act as a cross-linkage. Consequently, shortening of the distance between cross-linkages decreases the swelling ratio. In addition, it is possible that remaining lithium cations form coordination bonds with a few intramolecular sites, and the resultant increase in the stiffness of the chain also decreases the swelling ratio.

The swelling ratio increased with a decrease in n because the polymer chain could extend more freely, which is similar to a common tendency observed in typical hydrogels.

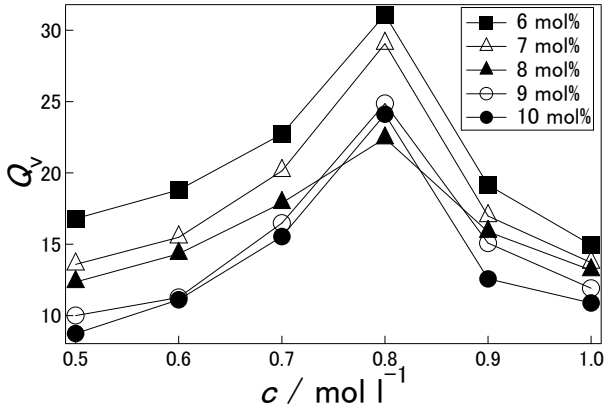

Fig. 4-3. Relationship between lithium ion density and the volume swelling ratio of HyPR-SR gels with various n; 10 mol% (●), 9 mol% (○), 8 mol% (▲),7 mol% (△) and 6 mol% (■).

4.3.3. Ionic conductivity of pristine ES and SR gels containing ES

AC impedance measurements were conducted for ESs and HyPR-SR gels **1-30** containing ESs. Figure 4-4 shows Arrhenius plots for the ionic conductivity of HyPR-SR gels **1-30**. The ionic conductivities σ, shown in Fig. 4-4 do not consider the quantities of the ESs; therefore, to compare ionic conductivity of each ES without the polymer matrix, which does not contribute to ionic conduction, the molar conductivity Λ, was calculated according to:

$$\Lambda = \sigma / \{c_0(1-\varphi_V)\}, \quad (3)$$

where φ_V is the volume fraction of ES, and c_0 is the sum of the molar concentration of lithium ions and IL. Table 4-3 shows σ, Λ, and the activation energies E_a, which were calculated from the slopes in Fig. 4-4, and the molar conductivity ratios of Λ to

the molar conductivity of pristine ES for HyPR-SR gels with various n swollen with various ESs with c. Figure 4-5(a) shows the relation between c and σ, and Fig. 4-5(b) shows the relation between c and Λ. Λ was smaller than Λ_0 and decreased with increasing n, while E_a for the HyPR-SR gel was larger than E_a for pristine ES. These results confirmed that the polymer matrix disturbs the ionic transport in the ES. The tendency for the ionic conductivity was similar to the swelling behavior shown in Fig. 4-5(a). The HyPR-SR gel had a maximum ionic conductivity at 0.8 M, although the ionic conductivity of the pristine ES decreased with an increase in the lithium ion density. In contrast, the molar conductivity showed a different tendency from ionic conductivity at low lithium ion density in Fig. 4-5(b). Although the calculated Λ values were revised with respect to φ_v, Λ for low lithium ion density at 0.5, 0.6 and 0.7 M was smaller than Λ for 0.8 M, in contrast to Λ_0. This suggests that φ_v with low lithium ion density is quite small, i.e., the polymer mesh was not extended to transport ionic carriers freely without disturbing the polymer mesh. In addition, at high lithium ion density, it was noted that the viscosities of the ESs included in the gels had a significant effect on the ionic transport.

(a)

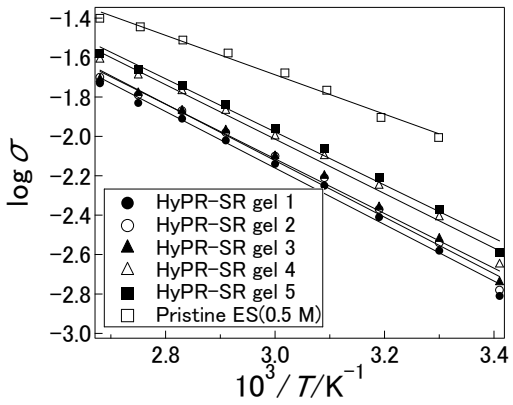

(b)

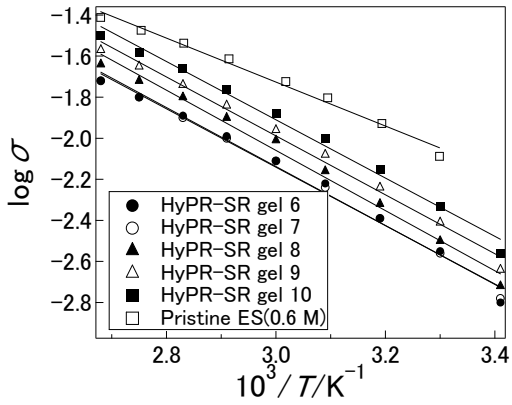

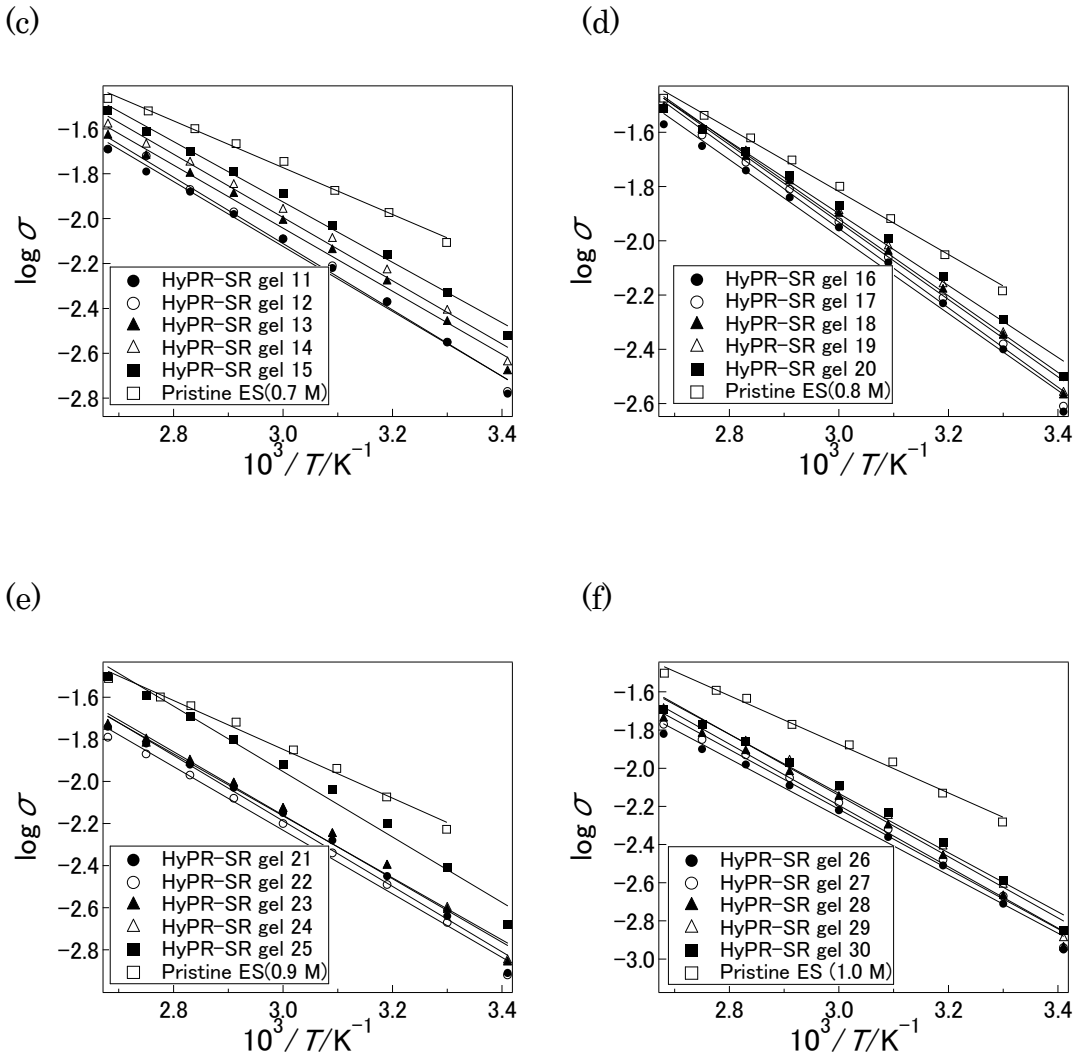

Fig. 4-4. (a) Arrhenius plots for HyPR-SR gel **1** (●), HyPR-SR gel **2** (○), HyPR-SR gel **3** (▲), HyPR-SR gel **4** (△), HyPR-SR gel **5** (■) and 0.5 M ES (□). (b) Arrhenius plots for HyPR-SR gel **6** (●), HyPR-SR gel **7** (○), HyPR-SR gel **8** (▲), HyPR-SR gel **9** (△), HyPR-SR gel **10** (■) and 0.6 M ES (□). (c) Arrhenius plots for HyPR-SR gel **11** (●), HyPR-SR gel **12** (○), HyPR-SR gel **13** (▲), HyPR-SR gel **14** (△), HyPR-SR gel **15** (■) and 0.7 M ES (□). (d) Arrhenius plots for HyPR-SR gel **16** (●), HyPR-SR gel **17** (○), HyPR-SR gel **18** (▲), HyPR-SR gel **19** (△), HyPR-SR gel **20** (■) and 0.8 M ES (□). (e) Arrhenius plots for HyPR-SR gel **21** (●), HyPR-SR gel **22** (○), HyPR-SR gel **23** (▲), HyPR-SR gel **24** (△), HyPR-SR gel **25** (■) and 0.9 M ES (□). (f) Arrhenius plots for HyPR-SR gel **26** (●), HyPR-SR gel **27** (○), HyPR-SR gel **28** (▲), HyPR-SR gel **29** (△), HyPR-SR gel **30** (■) and 1.0 M ES (□).

Table 4-3. Lithium ion density c, conductivity σ, molar conductivity Λ, and ratio of Λ to the molar conductivity of pristine ES (Λ_0) for SR gels swollen by ES to equilibrium with various cross-linking reagent number ratios n, at 303 K, and activation energy ΔE_a, estimated from the slope of Arrhenius plots.

c / mol L^{-1}	No.	σ / mS cm^{-1}	Λ / S cm^2 mol^{-1}	Λ / Λ_0 / %	ΔEa / kJ mol^{-1}
0.5	Pristine ES	9.87	4.55	100	8.32
	HyPR-SR gel **1**	2.66	1.61	35.4	11.2
	HyPR-SR gel **2**	2.91	1.51	33.1	11.5
	HyPR-SR gel **3**	3.05	1.86	40.9	11.5
	HyPR-SR gel **4**	3.88	2.19	48.1	12.0
	HyPR-SR gel **5**	4.31	2.35	51.4	11.9
0.6	Pristine ES	8.16	3.60	100	8.90
	HyPR-SR gel **6**	2.83	1.51	41.9	12.0
	HyPR-SR gel **7**	2.77	1.44	40.0	11.8
	HyPR-SR gel **8**	3.14	1.61	44.7	12.2
	HyPR-SR gel **9**	3.92	2.00	55.6	11.9
0.6	HyPR-SR gel **10**	4.67	2.34	65.0	11.8
0.7	Pristine ES	7.82	3.30	100	8.66
	HyPR-SR gel **11**	2.79	1.43	43.3	11.8
	HyPR-SR gel **12**	2.83	1.41	42.7	11.7
	HyPR-SR gel **13**	3.54	1.66	50.3	11.5
	HyPR-SR gel **14**	3.87	1.91	57.9	11.7
	HyPR-SR gel **15**	3.45	2.29	69.4	11.2
0.8	Pristine ES	6.54	2.65	100	9.65

c / mol L^{-1}	No.	σ / mS cm^{-1}	Λ / S cm^2 mol^{-1}	Λ/Λ_0 / %	$\triangle Ea$ / kJ mol^{-1}
0.8	HyPR-SR gel **16**	4.02	1.81	68.3	11.8
	HyPR-SR gel **17**	4.16	1.83	69.0	12.1
	HyPR-SR gel **18**	4.44	1.98	74.7	11.9
	HyPR-SR gel **19**	4.63	2.04	77.0	11.8
	HyPR-SR gel **20**	5.13	2.29	86.4	11.1
0.9	Pristine ES	5.92	2.30	100	9.64
	HyPR-SR gel **21**	2.11	1.03	44.8	12.9
	HyPR-SR gel **22**	2.28	9.92×10^{-1}	43.1	13.0
	HyPR-SR gel **23**	2.43	1.08	47.0	12.7
	HyPR-SR gel **24**	2.49	1.08	47.0	13.3
	HyPR-SR gel **25**	3.86	1.66	72.2	12.6
1.0	Pristine ES	5.23	1.96	100	10.6
	HyPR-SR gel **26**	1.96	9.14×10^{-1}	46.6	12.7
	HyPR-SR gel **27**	2.11	9.78×10^{-1}	49.9	12.9
	HyPR-SR gel **28**	2.16	9.46×10^{-1}	48.3	13.2
	HyPR-SR gel **29**	2.47	1.06	54.1	13.4
	HyPR-SR gel **30**	2.60	1.12	57.1	13.6

(a)

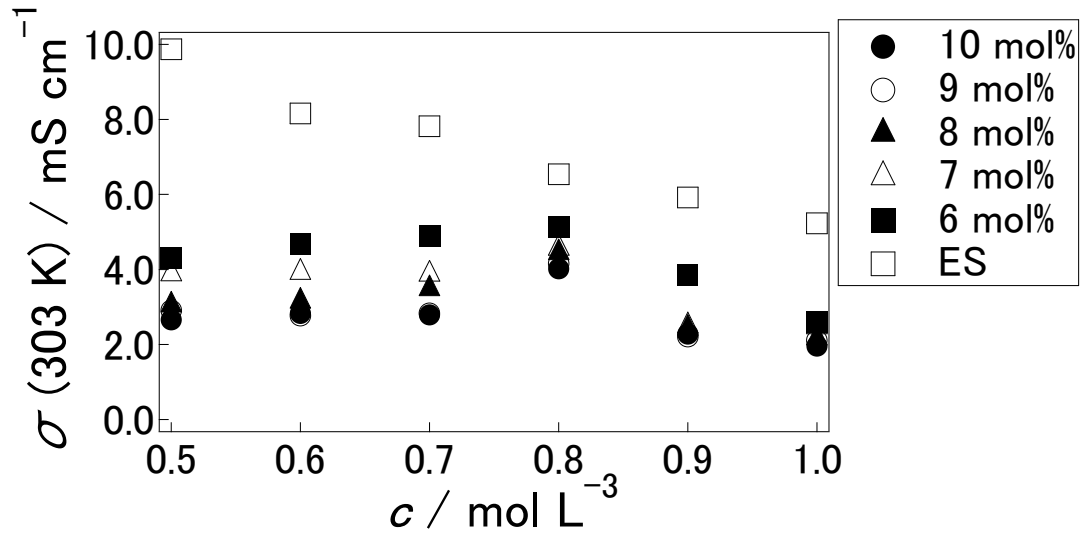

(b)

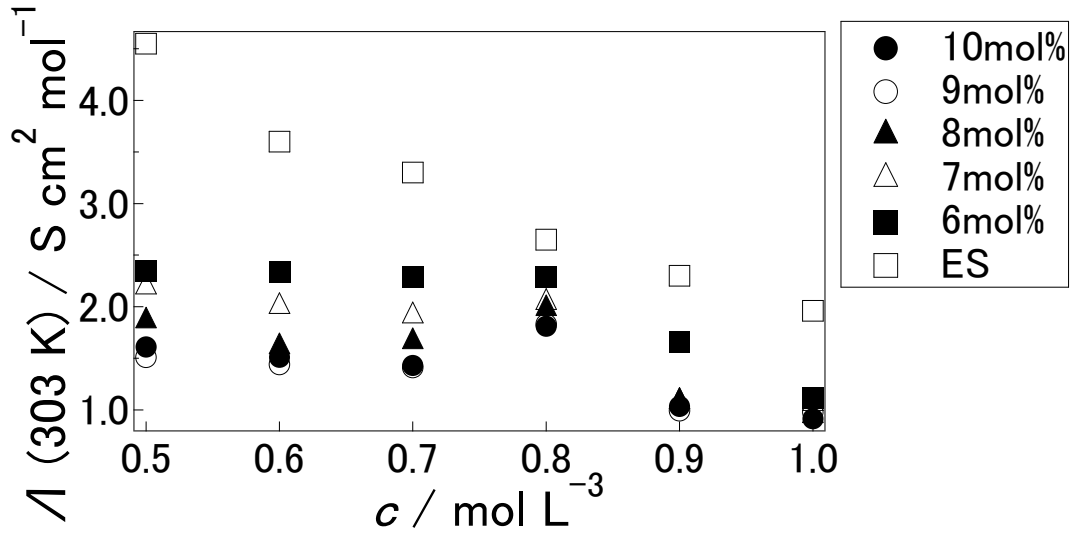

Fig. 4-5. (a) Relationship between lithium ion density and the ionic conductivity of HyPR-SR gels with various cross-linking reagent number ratios; 10 mol% (●), 9 mol% (○), 8 mol% (▲),7 mol% (△), 6 mol% (■) and ESs with various lithium ion densities (□). (b) Relationship between lithium ion density and the molar conductivity of HyPR-SR gels with various cross-linking reagent number ratio; 10 mol% (●), 9 mol% (○), 8 mol% (▲),7 mol% (△) and 6 mol% (■).

4.3.4. Puncture measurement of swollen SR gels containing ES

The mechanical properties of GPEs are closely dependent on the polymer network and GPEs with a large quantity of ES have been reported to be fragile [16-17]. However, in chapter 3.2.5, we investigated that GPEs based on SR gel with a large quantity of ES have been reported to have good mechanical properties due to their unique structure. The puncture stress is the maximum stress that the GPE can endure until the pin penetrates the GPE completely. Puncture measurements were performed 2-5 times on the same sample and the puncture stress and puncture elongation were estimated from the averaged peak of the stress-strain curve. Table 4-4 shows c, Q_v, the puncture elongation ε, and puncture stress σ_t, for the HyPR-SR gels. Figure 4-6(a) shows the relation between σ_t and ε for various c and Fig. 4-6(b) shows the relationship between c and Young's modulus, E. Both σ_t and E increased with the lithium ion density, which suggests that a pseudo and effective physical network is formed by the coordination of lithium ions in the SR gel, so that the SR GPE became harder and more fragile with increasing c. The SR gel has a unique mechanical property by the slide-ring effect where the cross-linking point can be moved freely on the axial polymer. The slide-ring effect imparts significant extensibility and swelling properties to the SR gel. Therefore, these SR GPEs exhibit large puncture elongations and high puncture stresses. In contrast, common gels become fragile with an increase in the quantity of ES and Q_v for these HyPR-SR gels increases with a decrease in n. However, n did not affect σ_t and ε, which indicates a weak relationship of $\sigma_t$and ε that can be ascribed to the enlarged polymer mesh with equilibrium swelling. On the other hand, in previous studies, reported ε of PVdF was less than 1.7 [18], hence these SR gels showed the higher

elongation than general gels.

Table 4-4. Lithium ion density c, volume swelling ratio Q_v, puncture elongation ε, and puncture stress, σ for the HyPR-SR gels.

c / mol L^{-1}	No.	Q_v of ES	ε	σ_t / N mm^{-2}
0.5	HyPR-SR gel **1**	4.2	17.4	9.16×10^{-2}
	HyPR-SR gel **2**	9.1	35.0	1.23×10^{-1}
	HyPR-SR gel **3**	4.1	31.0	1.72×10^{-2}
	HyPR-SR gel **4**	5.4	32.6	7.90×10^{-3}
	HyPR-SR gel **5**	6.4	17.0	1.50×10^{-1}
0.6	HyPR-SR gel **6**	5.8	23.9	16.1
	HyPR-SR gel **7**	6.5	17.6	7.36
	HyPR-SR gel **8**	7.2	16.3	75.0
	HyPR-SR gel **9**	7.3	18.2	4.07
	HyPR-SR gel **10**	8.3	18.6	8.16
0.7	HyPR-SR gel **11**	5.9	20.5	3.57
0.8	HyPR-SR gel **16**	9.7	14.0	6.02
	HyPR-SR gel **17**	12.5	27.9	6.12
	HyPR-SR gel **18**	11.1	29.9	8.44
	HyPR-SR gel **19**	10.4	21.8	3.57
	HyPR-SR gel **20**	10.9	24.4	5.29
0.9	HyPR-SR gel **21**	7.3	30.7	11.2
	HyPR-SR gel **22**	7.6	19.2	7.98
	HyPR-SR gel **24**	9.5	22.2	8.64
	HyPR-SR gel **25**	10.6	21.6	7.25
1.0	HyPR-SR gel **26**	5.1	16.9	9.25×10^{-1}
	HyPR-SR gel **27**	5.2	17.7	9.01×10^{-1}
	HyPR-SR gel **28**	7.1	18.4	8.26
	HyPR-SR gel **29**	7.6	12.4	1.75
	HyPR-SR gel **30**	7.7	19.0	1.42

(a)

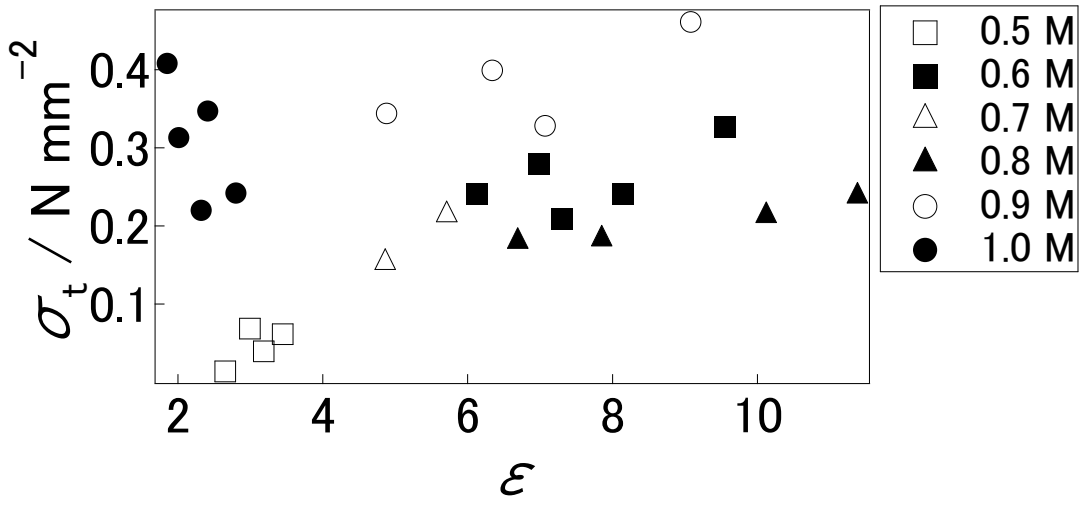

(b)

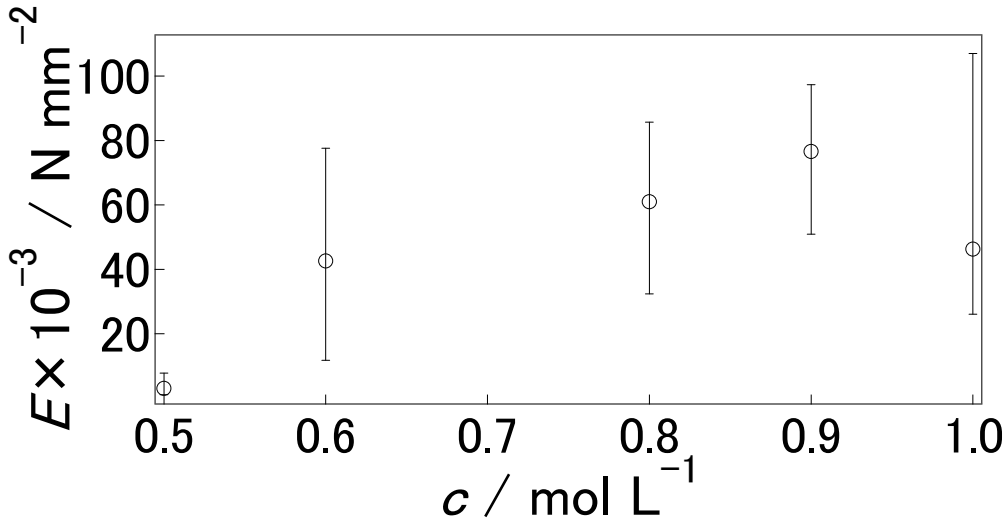

Fig. 4-6. (a) Puncture stress and puncture elongation for HyPR-SR gels swollen with various ESs of 1.0 M (●), 0.9 M (○), 0.8 M (▲), 0.7 M (△), 0.6 M (■) and 0.5 M (□). (b) Relationship between lithium ion density and Young's modulus.

In addition, puncture measurements were conducted for the non-equilibrium swollen HyPR-SR **31-38** gels with various swelling time. Table 4-5

shows the swelling time, ε, σ_t and E for HyPR-SR **31-38** gels, and Fig. 4-8 shows the relation between the swelling time, ε, and σ_t. HyPR-SR gel **31** had a low ε and high σ_t because this gel was a dry film. σ_t and E decreased with swelling time to reach equilibrium swelling. ε for HyPR-SR gel **32** was larger than that for the other HyPR-SR **33-38** gels.

Table 4-5. Swelling time, puncture strain ε, puncture stress σ, and Young's modulus E, for non-equilibrium swollen gels.

Swelling time / day	No.	ε	σ_t / N mm^{-2}	$E\times10^{-3}$ / N mm^{-2}
0	HyPR-SR gel **31**	5.16	30.8	60.5
1	HyPR-SR gel **32**	9.77	1.86	16.1
2	HyPR-SR gel **33**	5.86	3.80×10^{-1}	9.17
3	HyPR-SR gel **34**	4.39	2.56×10^{-1}	8.35
4	HyPR-SR gel **35**	6.03	8.43×10^{-1}	13.2
5	HyPR-SR gel **36**	7.33	9.02×10^{-1}	9.09
6	HyPR-SR gel **37**	5.67	4.64×10^{-1}	9.76
7	HyPR-SR gel **38**	7.51	9.82×10^{-1}	11.9

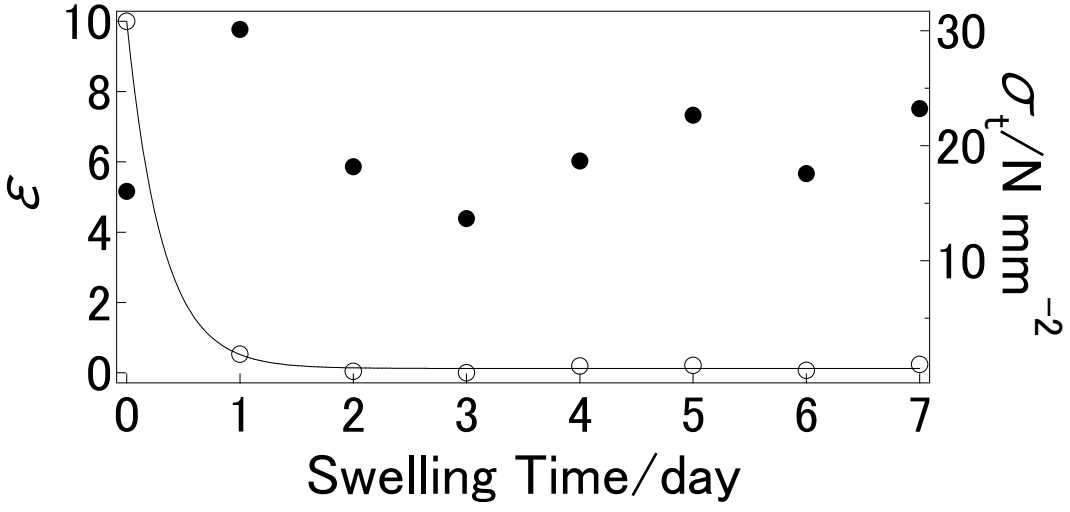

Fig. 4-8. Puncture stress and puncture elongation for non-equilibrium HyPR-SR swollen gels.

4.4. Summary

HyPR formed coordination bonds between lithium cations and ether oxygen atoms on HyCDs. The coordination bonds caused HyPR-SR gels to be swollen with an ES prepared from a lithium ion salt and hydrophobic IL. The swelling ratio and ionic conductivity of the HyPR-SR gel was the highest at a lithium ion density of 0.8 M, and the molar conductivity of HyPR-SR gel swollen with the 0.8 M ES was 85% more than that for the pristine ES. The puncture resistance, puncture stress and Young's modulus of the HyPR-SR gels increased with the lithium ion density, which suggested that pseudo and effective physical network was formed in the SR gel electrolyte.

References

[1] J. B. Bates, N. J. Dudney, B. Neudecker, A. Ueda. C. D. Evans, Thin-film lithium and lithium-ion batteries, Sol. St. Ion. 135 (2000) 33-45.

[2] T. Ohzuku, A. Ueda, M. Nagayama, Y. Iwakoshi, H. Komori, Comapative study of $LiCoO_2$, $LiNi_{12}Co_{12}O_2$ and $LiNiO_2$ for 4 volt secondary lithium sells, Electrochim. Acta 38 (1993) 1159-1167.

[3] Y. Y. Xia, M. Yoshio, An investigation of lithium ion insertion into spinel structure Li-Mn-O compounds, J. Electrochem. Soc. 143 (1996) 825-833.

[4] A. R. Armstrong, P. G. Bruce, Synthesis of layered $LiMnO_2$ as an electrode for rechargeable lithium batteries, Nature 381 (1996) 499-500.

[5] B. S. Kim, S. M. Park, In Situ spectroelectrochemical studies on the reduction of sulfur in dimethyl sulfoxide solutions, J. Electrochem. Soc. 140 (1993) 115-122.

[6] T. Sato, G. Masuda, K. Takagi, Electrochemical properties of novel ionic liquids for electronic duble layer capacitor applications, Electrochem. Acta 49 (2004) 3603-3611.

[7] A. Lewandowski, M. Galinski, Carbon-ionic liquid double-layer capacitors, J. Phys. Chem. Solids 65 (2004) 281-286.

[8] 大野弘幸監修 (2014) イオン液体Ⅱ-驚異的な進歩と多彩な近未来- <普及版> シーエム

シー出版
[9] J. M. Tarascon, M. Armand, Issues and facing rechargeable lithium batteries, Nature 414 (2001) 359-367.
[10] M. Armand, F. Endres, D. R. MacFarlane, H. Ohno, B. Scrosati, Ionic-liquid materials for the electrochemical challenges of the future, Nat. Mat. 8 (2009) 621-629.
[11] M. Park, X. C. Zhang, M. D. Chung, G. B. Less, A. M. Sastry, A review of conduction phenomena in Li-ion batteries, J. Power Sources 195 (2010) 7904-7929.
[12] A. Lewandowski, A. Swiderska-Mocek, Ionic liquids as electrolytes for Li-ion batteries-an overview of electrochemical studies, J. Power Sources 194 (2009) 601-609.
[13] J. Araki, K. Ito, Polyrotaxane derivatives. I. preparation of modified polyrotaxanes with nonionic functional groups and their solubility in organic solvent, J. Polym. Sci. 44 (2006) 6312-6323.
[14] S. Kanehashi, M. Kishida, T. Lidesaki, R. Shindo, S. Sato, T. Miyakoshi, K. Nagai, CO_2 separation properties of glassy aromatic polyimide composite membranes containing high-content 1-butyl-3-methylimidazolium bis(trifluoromethylsulfonyl)imide ionic liquid, J. Membr. Sci. 430 (2013) 211-222.
[15] L. Qiu, Z. Shao, M. Yang, W. Wang, F. Wang, J. Wan, J. Wang, Y. Bi, H, Duan, Study on effects of carboxymethyl cellulose lithium (CMC-Li) synthesis and electrospinning on high-rate lithium ion batteries, Cellulose 21 (2014) 615-626.
[16] Y. Wang, J. Travas-Sejdic, R. Steiner, Polymer gel electrolyte supported with mictroporous polyolefin membranes for lithium ion polymer battery, Sol. St. Ion. 148 (2002) 443-449.
[17] M. Wachtler, D. Ostrovskii, P. Jacobsson, B. Scrosati, A study on PVdF-based SiO_2-containig composite gel-type polymer electrolytes for lithium batteries, Electrochim. Acta 50 (2004) 357-361.
[18] Z. Jiang, B. Carroll, K. M. Abraham, Studies of poly(vinylidene fluoride) electrolyte, 42 (1997) 2667-2677.

Chapter 5

Conclusion

In my doctoral thesis, slide-ring (SR) gel, which was the novel kind of gel with a unique structure, have been investigated for applying to a gel polymer electrolyte by the slide-ring gel swollen with 1-ethyl-3-methylimidazolium ethylsulfate (EMIES), propylene carbonate (PC) including lithium bis(trifluoromethanesulfonyl)imide (LiTFSI) and 1-ethyl-3-methylimidazolium bis(trifluoromethanesulfonyl)imide (EMITFSI) including LiTFSI, respectively, in order to achieve the higher safety, high mechanical strength and high ionic conductivity.

In chapter 1 “Introduction”, the background of the research was introduced. The recent development and details of each component of lithium ion battery were described. Furthermore, the SR gels, which was the capital material of this research, was introduced in comparison with general gels.

In chapter 2 “Ionic Conduction and Mechanical Property of Slide-Ring Gels Swollen with Organic Liquid including Lithium Ions”, the swelling behavior with organic liquid including lithium ion, the electrochemical and mechanical properties were described. Methylated polyrotaxanes (MePR) were prepared with different degrees of substitution, and PR-SR gel and MePR-SR gel were obtained with changing cross-linking density. PR-SR gel was not swollen with pure PC and electrolyte solution (ES), which was 1.0 M PC of LiTFSI, because of making strong hydrogen bonding between each cyclodextrin. On the other hand, MePR-SR gel was swollen with PC and ES. This swelling behavior suggests that intermolecular hydrogen bonds between the methyl groups of MeCDs were broken by the formation of coordination bonds between lithium cations and ether oxygen on CDs. The molar conductivity of MePR-SR gel swollen with ES was more than 95 % of that of pristine

ES and the activation energy of MePR-SR gel swollen with ES was quite close to that of pristine ES, hence, it was concluded that this gel electrolyte had comparable properties to pristine ES. The potential window of MePR-SR gel swollen with ES suggests that SR gels do not affect potential window itself. In addition, the SR gel swollen with ES with high swelling ratio was not fractured under compression ratio of 50 % and had small young's modulus. This mechanical property suggests that the stress is uniformly dispersed and cracks are difficult to generate under high compression.

In chapter 3 "Ionic Conduction of Slide-Ring Gels Swollen with Ionic Liquids", the swelling behavior of the SR gel with ionic liquids, the ionic conduction, and the relationship between the ionic conductivity and mesh size of gel were investigated. SR gels, which were obtained from polyrotaxane (PR) and hydroxypropyl polyrotaxane (HyPR), were swollen with hydrophilic ILs, however, these SR gels was not swollen with hydrophilic ILs, and these tendencies suggested that the affinity of PEG and ILs was dominant in the swelling behavior. And the swelling ratio increased with decreasing cross-linking density. Furthermore, the ionic conductivities of SR gels swollen with EMIES were measured to compare the molar conductivity of SR gel containing IL and that of neat IL. The molar conductivity of SR gel containing IL was more than 92 % of that of neat IL, and the value decreased with swelling ratio. However, the value was higher than general gel containing IL, hence, disturbing of ion transport by polymer network in the SR gel was not influence under the high swelling ratio. And then, to investigate the hindrance of ionic transport by polymer network, the ionic conductivity was investigated with varying the mesh sizes of SR gels and non-SR gel changing

compression ratio. The ratio of the ionic conductivity of both gels against that of neat IL increased with compression ratio in the low compression region. On the other hand, under high compression ratio, non-SR gel was crushed and SR gel was not crushed, in addition, the ratio of the ionic conductivity of SR gel against that of neat IL decreased with increasing compression ratio. This result suggests that the polymer network was spread out perpendicular to the compressed direction and ionic carriers were more freely without interference from the network under low compression ratio. Under high compression ratio, ionic carriers could not escape from the polymer network disturbing from the deformation of the polymer network along the compressed direction.

In chapter 4 “Ionic Conduction and Mechanical Property of Slide-Ring Gels Swollen with Ionic Liquid including Lithium Ions”, the structure analysis of SR gel containing IL including lithium ion by ATR, the ionic conductivity with several lithium ion concentrations, and the mechanical strength by puncture measurement were investigated. The result of ATR-IR suggests that in HyPR coordination bonds between lithium cations and ether oxygen atoms on HyCDs were formed, and the coordination bonds let to the HyPR-SR gel swollen with ES, which was the mixture of hydrophobic IL and lithium ion. The swelling ratio and ionic conductivity showed the maximum peak at a lithium ion density of 0.8 M. The tendency of swelling ratio suggests that a solvation effect by formation of coordination bonds between HyPR and lithium cation in the IL below 0.8 M. On the other hand, above 0.8 M, decreasing swelling ratio by forming physical cross-linkages between PR matrices by lithium cations was suggested. In addition, the puncture stress and Young’s modulus of HyPR-SR gel swollen with ES increased with lithium ion density, which

suggested that pseudo and effective network was formed in the SR gel electrolyte.

From the above, the basic research of SR gel applying to gel polymer electrolyte was performed. SR gel showed the possibility of a new material for gel polymer electrolyte, which has both high ionic conductivity and high mechanical strength, and it is suggested that the SR gel electrolyte do not only achieve to development of lithium ion battery with higher safety and performance but enable to develop new batteries like flexible battery.

List of publications

List of Papers Related to This Research

[1] T. Moriyasu, T. Sakamoto, N. Sugihara, Y. Sasa, Y. Ota, T. Shimomura, Y. Sakai and K. Ito.

"Ionic Conduction of Slide-Ring Gel Swollen with Ionic Liquids."

Polymer, 54 (2013) 1490-1496.

[2] N. Sugihara, Y. Tominaga, T. Shimomura and K. Ito.

"Ionic Conductivity and Mechanical Properties of Slide-Ring Gel Swollen with Electrolyte Solution Including Lithium Ions"

Electrochimica Acta, 169 (2015) 433-439.

[3] N. Sugihara, K. Nishimura, H. Nishino, S. Kanehashi, K. Mayumi, Y. Tominaga, T. Shimomura and K. Ito.

"Ion-Conductive and Elastic Slide-Ring Li Electrolytes Swollen with Ionic Liquid"

Electrochimica Acta, Accepted.

List of International Conference Presentation

[1] N. Sugihara, S. Kanehashi, K. Mayumi, Y. Tominaga, T. Shimomura and K. Ito.
"Measurement of Ionic Conductivity and Mechanical Property of Slide-ring Gel Swollen with Propylene Carbonate including Lithium Ions"
The joint international meeting of: 2016 Fall Meeting of The Electrochemical Society of Japan - PRiME 2016 (2016)

List of Japanese Conference Presentations

[1] 坂本拓真，杉原直樹，下村武史，伊藤耕三
"電解質膨潤スライドリングゲルの構造と物性"
平成 24 年度繊維学会年次大会（2012）

[2] 杉原直樹，太田豊，下村武史
"スライドリングゲルを用いた高分子ゲル電解質の開発"
第 61 回高分子討論会（2012）

[3] 杉原直樹，太田豊，下村武史，伊藤耕三
"スライドリングゲルを用いた高分子ゲル電解質の開発"
平成 24 年度繊維学会年次大会（2013）

[4] 杉原直樹, 酒井康博, 富永洋一, 下村武史, 伊藤耕三

“リチウムイオン電解液による膨潤スライドリングゲルのイオン伝導率測定”

第 63 回高分子学会年会（2014）

[5] 杉原直樹, 酒井康博, 富永洋一, 下村武史, 伊藤耕三

“リチウムイオンで電解液膨潤させたスライドリングゲルの開発”

第 63 回高分子討論会（2014）

[6] 杉原直樹, 富永洋一, 下村武史, 伊藤耕三

“リチウムイオン含有イオン液体による膨潤スライドリングゲルのイオン伝導率測定”

第 64 回高分子学会年会（2015）

[7] 杉原直樹, 富永洋一, 下村武史, 伊藤耕三

“リチウムイオン含有電解液膨潤スライドリングゲルの イオン伝導率・力学特性”

平成 27 年度繊維学会年次大会（2015）ポスター賞受賞

[8] 杉原直樹, 眞弓皓一, 富永洋一, 下村武史, 伊藤耕三

“リチウムイオン含有炭酸プロピレンによる膨潤スライドリングゲルのイオン伝導率と力学特性”

2015 年電気化学会秋季大会（2015）

[9] 杉原直樹, 眞弓皓一, 富永洋一, 下村武史, 伊藤耕三

“リチウムイオン電解液膨潤スライドリングゲルのイオン伝導率と力学測定”

第 64 回高分子討論会（2015）

[10] Naoki SUGIHARA, Shinji KANEHASHI, Koichi MAYUMI, Yoichi TOMINAGA, Takeshi SHIMOMURA, Kohzo ITO

“Ionic Conduction Dependence on Lithium-Ion Density of Slide-ring Gel Electrolyte”

第 65 回高分子学会年会（2016）

Acknowledgements

My research was aided by many people surrounded me and I could continue my research and

Primary, I would like to express the deepest appreciation to Prof. Takeshi Shimomura who supported me since I assigned to Shimomura laboratory 6 years ago, for his leading on the works and my daily life. I will not forget the debt of gratitude that he does not guide me but talk to me the acquaintanceship of scientist and member of society at the formal and casual places.

I am also indebt to assistant Prof. Shinji Kanehashi for their helpful advices and suggestions in general such as analyzing data and writing papers.

For writing this thesis, four sub-adviser, Prof. Hiroaki Usui, Prof. Hiromu Saito, Associate Prof. Hideaki Oike, Associate Prof. Yoichi Tominaga, gave so much insightful comments and suggestions. Their valuable comments made this thesis more sophisticated one.

Members of Shimomura laboratory, Mr. Taiki Ito, Mr. Hikari Narita, Mr. Morito Yagi, Ms. Haruka Nishino, Ms. Mitsuko Motoyama, Mr. Naoki Okada, Ms. Moe Okada, Mr. Takanori Goto, Mr. Surendra Babu Anantharaman, warmed up the laboratory, so I had a good time.

All members of Tominaga laboratory were supported my experiments. If there are not them helps, I cannot write this thesis.

Finally I would also like to express the deepest appreciation to my both parents and my friends for mental supports.